



RESEARCH ARTICLE

10.1029/2018GB005968

Key Points:

- A food web model for the Costa Rica Dome is constrained by measured process rates and  $\delta^{15}\text{N}$
- Mesozooplankton trophic dynamics with large fluxes from protistivory and detritivory are central to the functioning of the biological pump
- Active transport by diel vertically migrating mesozooplankton contributes 36–46% of total export

Supporting Information:

- Supporting Information S1
- Table S1
- Data Set S1

Correspondence to:

M. R. Stukel,  
mstukel@fsu.edu

Citation:

Stukel, M. R., Décima, M., Landry, M. R., & Selph, K. E. (2018). Nitrogen and isotope flows through the Costa Rica Dome upwelling ecosystem: The crucial mesozooplankton role in export flux. *Global Biogeochemical Cycles*, 32. <https://doi.org/10.1029/2018GB005968>

Received 30 APR 2018

Accepted 30 NOV 2018

Accepted article online 5 DEC 2018

# Nitrogen and Isotope Flows Through the Costa Rica Dome Upwelling Ecosystem: The Crucial Mesozooplankton Role in Export Flux

Michael R. Stukel<sup>1,2</sup> , Moira Décima<sup>3</sup>, Michael R. Landry<sup>4</sup>, and Karen E. Selph<sup>5</sup>

<sup>1</sup>Department of Earth, Ocean, and Atmospheric Science, Florida State University, Tallahassee, FL, USA, <sup>2</sup>Center for Ocean-Atmospheric Prediction Studies, Florida State University, Tallahassee, FL, USA, <sup>3</sup>National Institute of Water and Atmospheric Research, Wellington, New Zealand, <sup>4</sup>Scripps Institution of Oceanography, University of California, San Diego, La Jolla, CA, USA, <sup>5</sup>Department of Oceanography, University of Hawaii at Mānoa, Honolulu, HI, USA

**Abstract** The Costa Rica Dome (CRD) is an open-ocean upwelling ecosystem, with high biomasses of picophytoplankton (especially *Synechococcus*), mesozooplankton, and higher trophic levels. To elucidate the food web pathways supporting the trophic structure and carbon export in this unique ecosystem, we used Markov Chain Monte Carlo techniques to assimilate data from four independent realizations of  $\delta^{15}\text{N}$  and planktonic rate measurements from the CRD into steady state, multicompartiment ecosystem box models (linear inverse models). Model results present well-constrained snapshots of ecosystem nitrogen and stable isotope fluxes. New production is supported by upwelled nitrate, not nitrogen fixation. Protistivory (rather than herbivory) was the most important feeding mode for mesozooplankton, which rely heavily on microzooplankton prey. Mesozooplankton play a central role in vertical nitrogen export, primarily through active transport of nitrogen consumed in the surface layer and excreted at depth, which comprised an average 36–46% of total export. Detritus or aggregate feeding is also an important mode of resource acquisition by mesozooplankton and regeneration of nutrients within the euphotic zone. As a consequence, the ratio of passively sinking particle export to phytoplankton production is very low in the CRD. Comparisons to similar models constrained with data from the nearby equatorial Pacific demonstrate that the dominant role of vertical migrators to the biological pump is a unique feature of the CRD. However, both regions show efficient nitrogen transfer from mesozooplankton to higher trophic levels (as expected for regions with large fish, cetacean, and seabird populations) despite the dominance of protists as major grazers of phytoplankton.

**Plain Language Summary** Most of the world's oceanic regions can be divided into (1) low-nutrient areas where small algae dominate and crustaceans, fish, and whales are scarce or (2) productive areas where large algae dominate, crustaceans and higher trophic levels are abundant, and substantial carbon is transported to depth as part of the *biological pump*. The Costa Rica Dome (CRD) is a unique natural laboratory for investigating the relationships between algae, zooplankton, and marine biogeochemistry because it is a productive region dominated by cyanobacteria (small algae) that nevertheless sustains large populations of crustaceans, fish, and whales. We used a novel data assimilation tool to constrain a food web model using at-sea rate measurements of plankton activity and nitrogen stable isotopes. We found that protists are an important intermediate trophic level linking cyanobacteria and mesozooplankton. Efficient recycling by the zooplankton community facilitates nitrogen transfer to fish, whales, and seabirds. In the CRD, vertically migrating zooplankton (which feed in the surface during the night but descend to depth during the day to escape predators) play a particularly important role in transporting nitrogen (and carbon dioxide) from the surface to the deep ocean, where it can be removed from the atmosphere.

## 1. Introduction

The Costa Rica Dome (CRD) is a unique open ocean upwelling ecosystem in the eastern tropical Pacific (Fiedler, 2002; Hofmann et al., 1981; Landry, De Verneil, et al., 2016). While it has many similarities to the nearby upwelling center in the eastern equatorial Pacific (upwelling, high primary productivity and new production, high biomass of upper trophic levels, and potential micronutrient limitation), it also differs in some key ways (Figure 1). Most notably, despite the CRD being a highly productive system, its phytoplankton community is dominated by picophytoplankton, with the highest concentrations of *Synechococcus* (*SYN*) measured anywhere in the world ocean (Li et al., 1983; Saito et al., 2005; Taylor et al., 2016). The CRD and

©2018. The Authors.

This is an open access article under the terms of the Creative Commons Attribution-NonCommercial-NoDerivs License, which permits use and distribution in any medium, provided the original work is properly cited, the use is non-commercial and no modifications or adaptations are made.

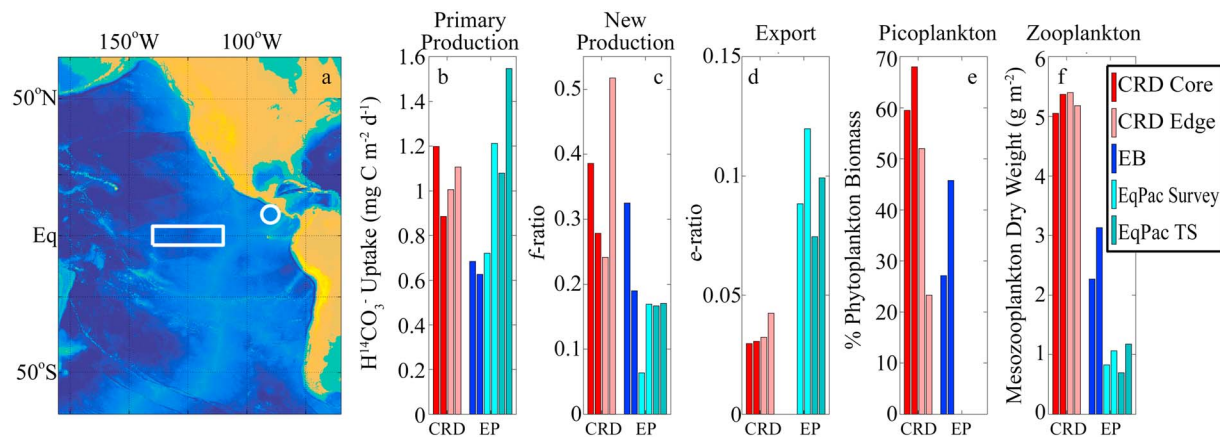


**Figure 1.** Comparison of results from Costa Rica Dome (CRD), equatorial biocomplexity (EB), JGOFS EqPac survey, and JGOFS EqPac time series (TS) cruises. (a) Study regions (circle is CRD, rectangle is equatorial Pacific). (b) Primary production (Balch et al., 2011; Barber et al., 1996; Taylor et al., 2016). (c)  $f$  ratio = new production/primary production (McCarthy et al., 1996; Parker et al., 2011; Stukel et al., 2016). (d)  $e$  ratio = export/primary production (Buesseler et al., 1995; Dunne et al., 2000; Stukel et al., 2016). (e) Picophytoplankton biomass/total phytoplankton biomass (Selph et al., 2011; Taylor et al., 2016, 2011). (f) Mesozooplankton biomass (Dam et al., 1995; Décima et al., 2011, 2016; Roman et al., 2002; Roman & Gauzens, 1997). Replicate bars are results from different Lagrangian experiments (CRD) and different cruises (EB and EqPac). JGOFS = Joint Global Ocean Flux Study; EqPac = equatorial Pacific.

eastern equatorial Pacific thus serve as an interesting contrast for assessing the importance of food web pathways (rather than system productivity) in structuring the biogeochemical fate of organic carbon fixed in the surface ocean.

The Flux and Zinc Experiments cruise in June–July 2010 was designed to investigate biogeochemical-ecological relationships in the CRD by quantifying community biomass structure, regulation of phytoplankton production by trace elements and grazing, and associated ecosystem fluxes (Landry, De Verneil, et al., 2016). Cruise results confirmed high primary productivity and a dominant role for SYN. However, some surprising results were also obtained. While new production and the  $f$  ratio (ratio of new production to total primary production) were high (in fact, higher than in the equatorial Pacific), sinking particle export was quite low, with export ratios ( $e$  ratio = export/primary productivity) less than 0.05 (Figures 1b–1d, Stukel et al., 2016). Also, despite the dominant role of SYN in the region, mesozooplankton biomass was substantially higher than in the equatorial Pacific (Dam et al., 1995; Décima et al., 2011, 2016; Roman et al., 2002). The food web structure and ecosystem pathways necessary to support this surprisingly low export and high mesozooplankton biomass are currently unknown and provide the motivation for the present constrained model analysis.

Nitrogen isotopic measurements are a powerful tool for understanding trophic dynamics for two reasons: (1) sources of nitrogen to the euphotic zone ecosystem often have distinct isotopic contents (e.g.,  $N_2$  fixation and upwelled  $NO_3^-$ ; Casciotti, 2016; Robinson, 2001) and (2) biochemical processes fractionate nitrogen leading to enrichment in  $^{15}N$  with increasing trophic levels (Montoya, 2008; Post, 2002).  $\delta^{15}N$  measurements have consequently been used to estimate the importance of  $N_2$  fixation supporting zooplankton biomass production or sinking particle flux (Dore et al., 2002; Montoya et al., 2002) and to quantify the food web structure in many marine ecosystems (Fleming et al., 2014; Hobson et al., 2002). However, interpretations of isotopic data can be confounded when ecosystem nitrogen source and trophic structure are both unknown or variable (Rau et al., 2003). Combining  $\delta^{15}N$  isotopic data with classical food web rate and standing stock measurements is thus likely to be a powerful approach for understanding carbon and nitrogen flows through an ecosystem.

In the present study, we use linear inverse ecosystem modeling (LIEM) techniques to combine a diverse array of in situ measurements of plankton rate processes and nitrogen biogeochemistry into a well-constrained depiction of the CRD marine ecosystem. LIEM is a powerful tool for assimilating ecological and biogeochemical rate and standing stock measurements into a coherent food web model (van Oevelen et al., 2010; Vézina & Platt, 1988). LIEM uses linear programming methods to constrain a system of equations including exact equalities representing mass balance constraints, approximate equalities representing in situ rate measurements with quantified uncertainties, and greater than/less than constraints representing bounded

physiological and ecological constraints on the ecosystem (van Oevelen et al., 2010; Vézina & Platt, 1988). Because of the large number of potential food web pathways and the paucity of in situ measurements, pelagic LIEMs are typically vastly underconstrained and hence potentially solved by an infinite number of scenarios that satisfy the linear constraints. Kones et al. (2009, 2006) developed a Markov Chain Monte Carlo (MCMC) approach to sample the solution space that satisfies the model constraints. They suggested the mean solution as a good approximate of ecosystem structure, and subsequent studies showed that the mean MCMC solution was a better predictor of withheld ecosystem measures than previously used  $L_2$  minimum norm approaches (Saint-Béat et al., 2013; Stukel et al., 2012). Here we use a novel implementation of MCMC sampling of the ecosystem (MCMC+ $^{15}\text{N}$ ) to incorporate nonlinear isotopic constraints into the ecosystem (Stukel et al., 2018). Using this data assimilation tool, we ask three basic questions: What trophic pathways support abundant mesozooplankton populations in the CRD despite picoplankton dominance in the autotrophic community? How do organic matter export processes balance the high new production rates measured in the CRD? How do differences in the planktonic communities of the CRD and equatorial Pacific affect the biogeochemical fates of biological production?

## 2. Methods

### 2.1. In Situ Measurements

Cruise measurements in the CRD were made in July 2010 following a weak El Niño, when dome expression (i.e., shoaling isopycnals) was depressed relative to climatological mean summer conditions (Landry, De Verneil, et al., 2016). The sampling program was designed around 4-day semi-Lagrangian experiments, referred to here as *cycles*, during which a satellite-tracked array with a mixed-layer drogue was deployed daily and used both to follow water parcels and as an experimental platform for in situ incubations at eight depths. A second Lagrangian array with VERTEX-style Particle Interceptor Trap (PIT) sediment traps was deployed for the full 4 days per cycle to collect sinking material and quantify export flux (Stukel, Décima, et al., 2013). This approach allowed repeated sampling of an evolving planktonic community and determination of net trajectories for integrated euphotic zone standing stocks (Landry et al., 2009; Landry, Selph, et al., 2016). Four cycle experiments were completed in waters representative of the dome from 4 to 24 July, each an independent realization of the ecosystem with broadly similar food web structure. A fifth coastal cycle was also completed at the beginning of the cruise, but due to its location and lack of primary productivity data, we do not include its results in this model analysis.

Cruise measurements included systematic sampling of the planktonic community from primary producers to mesozooplankton consumers (Table 1). Net primary production was measured daily by  $\text{H}^{14}\text{CO}_3^-$  uptake in triplicate samples incubated in situ at eight depths spanning the euphotic zone (Selph et al., 2016). Taxon-specific rates of phytoplankton growth and protozoan grazing were also quantified at eight depths in situ by two-point dilution experiments and subsequent sample analyses by high-pressure liquid chromatography (HPLC) for nanophytoplankton and microphytoplankton taxa and flow cytometry for picophytoplankton (Selph et al., 2016). Instantaneous estimates of growth and grazing rates were converted to carbon-based production and loss rates using standard cell-biomass conversion rates for picophytoplankton and epifluorescence microscopy-derived biomass estimates for the larger taxa (Landry, Selph, et al., 2016; Taylor et al., 2016). Here, we divide the phytoplankton taxa into *Prochlorococcus* (*PRO*), *SYN*, picoeukaryotes (*PEUK*), diatoms (*DTM*), and combined other nanophytoplankton and microphytoplankton. The latter group was composed primarily of flagellates that we assume were mixotrophic (Freibott et al., 2016; Stukel et al., 2011). Biomass of nonpigmented protists was quantified by a combination of epifluorescence microscopy for nanoflagellates and dinoflagellates and light microscopy for ciliates (Freibott et al., 2016). Mesozooplankton were sampled with paired day-night oblique net tows through the euphotic zone with a 1-m ring net with flow meter and time-depth recorder (Décima et al., 2016). The resulting samples were size fractionated (0.2–0.5, 0.5–1, 1–2, 2–5 and >5 mm) and split for biomass or gut fluorescence (herbivorous grazing) assessments. Here we divide the community into small (<1 mm) and large (>1 mm) zooplankton. A subset of the samples was also analyzed for  $\delta^{15}\text{N}$ . For each size class, we calculated daily grazing rates of nonvertical migrants as 24 times the daytime hourly grazing rate and grazing rates of vertical migrants as 12 times the difference between night and day grazing rates. For rates or standing stocks reported in carbon units, we converted to nitrogen units assuming a 106:16 C:N molar ratio for prokaryotes and protists and 100:23 for mesozooplankton (Landry et al., 2001).

**Table 1**

*In Situ Measurements From the CRD Cruise Lagrangian Experiments Conducted in the Core of the CRD (Cycles 2 and 4) and on the Periphery of the CRD (Cycles 3 and 5)*

Measurement	Cycle 2	Cycle 3	Cycle 4	Cycle 5	Source
$^{14}\text{C}$ Primary production ( $\text{mmol C}\cdot\text{m}^{-2}\cdot\text{day}^{-1}$ )	100 ± 26	84 ± 4	74 ± 18	92 ± 21	Selph et al. (2016)
<i>Prochlorococcus</i> production ( $\text{mmol C}\cdot\text{m}^{-2}\cdot\text{day}^{-1}$ )	9.1 ± 1.8	2.1 ± 0.4	4.3 ± 0.9	3.4 ± 0.7	Selph et al. (2016)
<i>Synechococcus</i> production ( $\text{mmol C}\cdot\text{m}^{-2}\cdot\text{day}^{-1}$ )	17.8 ± 3.6	7.3 ± 1.5	13.9 ± 2.8	5.3 ± 1.1	Selph et al. (2016)
Picoeukarote production ( $\text{mmol C}\cdot\text{m}^{-2}\cdot\text{day}^{-1}$ )	6 ± 1	13 ± 3	6 ± 1	6 ± 1	Selph et al. (2016)
Diatom production ( $\text{mmol C}\cdot\text{m}^{-2}\cdot\text{day}^{-1}$ )	0.4 ± 0.1	2.2 ± 0.4	3.2 ± 0.6	11.3 ± 2.3	Selph et al. (2016)
Protozoan grazing (total) ( $\text{mmol C}\cdot\text{m}^{-2}\cdot\text{day}^{-1}$ )	96 ± 36	54 ± 13	34 ± 9	38 ± 9	Landry, Selph, et al. (2016)
Protozoan grazing (Prochlo) ( $\text{mmol C}\cdot\text{m}^{-2}\cdot\text{day}^{-1}$ )	7.5 ± 1.5	2.1 ± 0.4	4.4 ± 0.9	2.8 ± 0.6	Landry, Selph, et al. (2016)
Protozoan grazing (Syn) ( $\text{mmol C}\cdot\text{m}^{-2}\cdot\text{day}^{-1}$ )	35.3 ± 7.1	12.1 ± 2.4	10.3 ± 2.1	5.7 ± 1.1	Landry, Selph, et al. (2016)
Protozoan grazing (picoeuk; $\text{mmol C}\cdot\text{m}^{-2}\cdot\text{day}^{-1}$ )	4.5 ± 0.9	8.4 ± 1.7	3 ± 0.6	3.8 ± 0.8	Landry, Selph, et al. (2016)
Protozoan grazing (diatom; $\text{mmol C}\cdot\text{m}^{-2}\cdot\text{day}^{-1}$ )	0.07 ± 0.01	0.35 ± 0.07	0.51 ± 0.1	1.83 ± 0.37	Landry, Selph, et al. (2016)
<1-mm non-DVM mesozoo grazing ( $\text{mmol C}\cdot\text{m}^{-2}\cdot\text{day}^{-1}$ )	15.2 ± 5.6	22.3 ± 6.9	11.1 ± 3.7	29.2 ± 10.8	Décima et al. (2016)
<1-mm DVM mesozoo grazing ( $\text{mmol C}\cdot\text{m}^{-2}\cdot\text{day}^{-1}$ )	5.4 ± 2.9	11.2 ± 7	1.1 ± 1	7.2 ± 4.2	Décima et al. (2016)
>1-mm non-DVM mesozoo grazing ( $\text{mmol C}\cdot\text{m}^{-2}\cdot\text{day}^{-1}$ )	7.5 ± 3.3	27 ± 7.9	6 ± 2.3	12.7 ± 4.2	Décima et al. (2016)
>1-mm DVM mesozoo grazing ( $\text{mmol C}\cdot\text{m}^{-2}\cdot\text{day}^{-1}$ )	3.4 ± 2.2	3.8 ± 6.1	2.2 ± 1.8	8.4 ± 4.8	Décima et al. (2016)
Nitrate uptake ( $\text{mmol N}\cdot\text{m}^{-2}\cdot\text{day}^{-1}$ )	5.8 ± 1.3	3.1 ± 0.4	3.1 ± 0.2	7.2 ± 0.9	Stukel et al. (2016)
Export flux at 50-m depth ( $\text{mmol N}\cdot\text{m}^{-2}\cdot\text{day}^{-1}$ )	0.45 ± 0.06	0.41 ± 0.03	0.34 ± 0.03	0.59 ± 0.04	Stukel et al. (2016)
<i>Prochlorococcus</i> biomass ( $\text{mmol C}/\text{m}^2$ )	22 ± 3.4	8.9 ± 2	19.2 ± 4.8	9.5 ± 3	Taylor et al. (2016)
<i>Synechococcus</i> biomass ( $\text{mmol C}/\text{m}^2$ )	52.9 ± 7.7	17.8 ± 1.3	30 ± 3.1	9.8 ± 2.9	Taylor et al. (2016)
Picoeukaryote biomass ( $\text{mmol C}/\text{m}^2$ )	17.3 ± 1.6	20.5 ± 3.7	13.2 ± 0.7	11.6 ± 1.9	Taylor et al. (2016)
Diatom biomass ( $\text{mmol C}/\text{m}^2$ )	0.6 ± 0.2	1.6 ± 0.6	1.7 ± 0.4	2.6 ± 0.1	Taylor et al. (2016)
Other phytoplankton biomass ( $\text{mmol C}/\text{m}^2$ )	64.3 ± 11.6	47 ± 3.4	37.7 ± 5.6	95.4 ± 21.1	Taylor et al. (2016)
Heterotrophic nanoflagellate biomass ( $\text{mmol C}/\text{m}^2$ )	25.2 ± 5.5	27 ± 6.5	20.9 ± 3.2	25 ± 0	Freibott et al. (2016)
Microzooplankton biomass ( $\text{mmol C}/\text{m}^2$ )	18.7 ± 6.6	18.1 ± 4.5	20.9 ± 7	18.4 ± 0	Freibott et al. (2016)
<1-mm non-DVM mesozoo biomass ( $\text{mmol C}/\text{m}^2$ )	52.3 ± 6.2	76.8 ± 16.7	64.8 ± 12.2	72 ± 5.1	Décima et al. (2016)
<1-mm DVM mesozoo biomass ( $\text{mmol C}/\text{m}^2$ )	26.4 ± 8.1	20.5 ± 27	32.4 ± 13.2	34 ± 9.2	Décima et al. (2016)
>1-mm non-DVM mesozoo biomass ( $\text{mmol C}/\text{m}^2$ )	51.7 ± 9.2	53.4 ± 11.2	42.4 ± 6.7	57.2 ± 21.7	Décima et al. (2016)
>1-mm DVM mesozoo biomass ( $\text{mmol C}/\text{m}^2$ )	96.7 ± 12.1	79.2 ± 35.7	110 ± 19.6	39.3 ± 27.7	Décima et al. (2016)
Particulate nitrogen ( $\text{mmol N}/\text{m}^2$ )	103 ± 7	90 ± 3	80 ± 2	69 ± 6	Stukel et al. (2016)
Vertical gradient particulate nitrogen ( $\text{mmol N}/\text{m}^4$ )	-0.04 ± 0.01	-0.03 ± 0	-0.02 ± 0.01	-0.02 ± 0.01	Stukel et al. (2016)
$\delta^{15}\text{N}$ $\text{NO}_3^-$ (euphotic zone)	10.3	12.7	9.9	11.5	Buchwald et al. (2015)
$\delta^{15}\text{N}$ $\text{NO}_3^-$ (50–100 m)	7.6	5.7	6.6	6.6	Buchwald et al. (2015)
$\delta^{15}\text{N}$ particulate nitrogen (euphotic zone)	3.9	5.8	4.9	5.2	Stukel et al. (2016)
$\delta^{15}\text{N}$ sinking particles	7.9 <sup>a</sup>	4.6	5.3	6.9	Stukel et al. (2016)
$\delta^{15}\text{N}$ < 1-mm mesozooplankton	8.8	9.4	9	9.1	Décima et al. (2019)
$\delta^{15}\text{N}$ > 1-mm mesozooplankton	9.9	10	10	9.8	Décima et al. (2019)
Temperature (euphotic zone, °C)	21.7	23.4	23	24.9	CTD
Temperature (beneath euphotic zone, °C)	11.8	11.8	11.8	12.7	CTD

Note. Means ± standard error. CRD = Costa Rica Dome; CTD = Conductivity, Temperature, Depth; DVM = diel vertical migration.

<sup>a</sup>For calculation of Cycle 2 sediment trap  $\delta^{15}\text{N}$ , we excluded one outlier with anomalously high  $\delta^{15}\text{N}$ .

Biogeochemical rate measurements included  $^{15}\text{NO}_3^-$  uptake measurements conducted at eight depths on the in situ array (Stukel et al., 2016). Because nitrification rate measurements indicate that  $\text{NO}_3^-$  regeneration in the euphotic zone was negligible (~0.1% of nitrate uptake), we conclude that  $\text{NO}_3^-$  uptake represented new production (Buchwald et al., 2015; Stukel et al., 2016). We measured carbon and nitrogen fluxes of sinking particles into VERTEX-style sediment traps deployed at depths of 90 and 150 m on the sediment trap array (Stukel, Décima, et al., 2013; Stukel et al., 2016). Vertical profiles of  $^{234}\text{Th}$ - $^{238}\text{U}$  deficiency were measured twice per cycle and confirmed that there was no substantial overcollection or undercollection of sinking material by the sediment traps. This does not, however, exclude the possibility that sinking organic matter with low  $^{234}\text{Th}$  activity (i.e., high C: $^{234}\text{Th}$  ratios), including mesozooplankton and fecal material of higher organisms, may have been undersampled by the traps, while contributing substantially to carbon flux (Stukel et al., 2016).  $\delta^{15}\text{N}$  values were measured for sinking particles and bulk suspended particulate organic matter (POM) in the water column, and the  $\delta^{15}\text{N}$  of  $\text{NO}_3^-$  beneath the euphotic zone was determined by the denitrifier method (Buchwald et al., 2015; Stukel et al., 2016). Further details of data manipulation for inclusion as constraints on the inverse model are in the online Appendix (Childress et al., 1980; Conover, 1966; Del Giorgio & Cole, 1998; Eichinger et al., 2006; Houde & Schekter, 1983; Ikeda, 1985; Soetaert et al., 2009; Vézina & Pahlow, 2003).

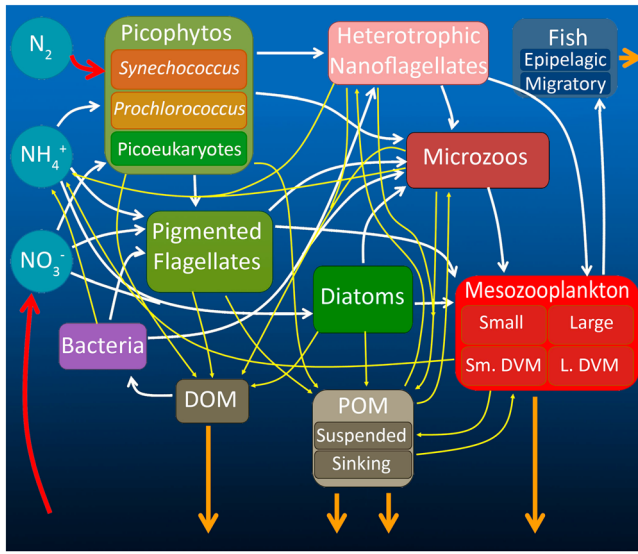


**Figure 2.** Conceptual model of nitrogen fluxes via trophic flows (white), flows involving detritus and nutrient regeneration (yellow), new production flows (red), and export flows (orange). This diagram agglomerates model compartments that behave similarly (e.g., all picophytoplankton or all mesozooplankton) and hence has fewer flows than the full model (supporting information Table S1). DOM = dissolved organic matter; POM = particulate organic matter.

## 2.2. Inverse Ecosystem Model Structure

Primary producers in the inverse model comprise picophytoplankton (subdivided into PRO, SYN, and PEUK), DTM, and other nanophototrophs or microphototrophs (AUT), which we assumed are mixotrophic. In addition to AUT, modeled grazers include heterotrophic nanoflagellates, microzooplankton, small (<1 mm) nonvertically migrating mesozooplankton, small vertically migrating mesozooplankton, large nonvertically migrating mesozooplankton, and large vertically migrating mesozooplankton. Mesozooplankton secondary production is consumed by epipelagic fish or vertically migrating fish. Bacteria remineralize dissolved organic matter (DOM) to  $\text{NH}_4^+$ . Nonliving POM is separated into two classes including suspended detritus (DET) and large sinking detritus. New production includes  $\text{NO}_3^-$  uptake (by all phytoplankton classes) and nitrogen fixation, which we assumed is mediated by unicellular cyanobacteria group B containing phycoerythrin and hence would likely be classified as SYN by our flow cytometric measurements (*Trichodesmium* was not observed on the cruise). New production is balanced by six export terms: sinking of detritus and fish fecal pellets, physical transport (mixing or subduction) of DOM and DET, active transport by vertically migrating mesozooplankton and vertically migrating fish, and fish secondary production. From extensive microscopic analyses of sediment trap contents that did not efficiently sample fish fecal pellets, we assume that the fish contribution to export is in addition to the sediment trap measured export. All flows in the model are in N currency ( $\text{mmol N}\cdot\text{m}^{-2}\cdot\text{day}^{-1}$ ), depicted in Figure 2 and explained in supporting information Table S1.

## 2.3. Inverse Ecosystem Model Solution

To determine the most representative solutions and uncertainty estimates for the underconstrained inverse models, we use a modified version of the MCMC sampling method (Kones et al., 2009; Van den Meersche et al., 2009; van Oevelen et al., 2010). This approach involves a set of exact equalities ( $\text{Ex} = \text{f}$ ) that represent mass balance constraints on every compartment in the ecosystem, a set of approximate equalities ( $\text{Ax} \approx \text{b}$ ) that include the measured constraints on the ecosystem with measurement uncertainties, and a set of inequalities ( $\text{Gx} \geq \text{h}$ ) that include known constraints on components of the ecosystem. In each of these equations, the vector  $\text{x}$  represents the 116 unknown nitrogen flows through the ecosystem that we wish to constrain (Figure 2 and supporting information Table S1).  $\text{E}$  is a  $19 \times 116$  matrix of ones, zeroes, and negative ones that codifies mass balance constraints, and  $\text{f}$  is a  $19 \times 1$  vector of zeroes because we assume steady state.  $\text{A}$  is a  $41 \times 116$  matrix (and  $\text{b}$  is a  $41 \times 1$  vector) that both vary depending on the in situ data. Together,  $\text{A}$  and  $\text{b}$  represent the 21 rate measurement constraints measured in situ and  $20^{15}\text{N}$  isotope mass balances.  $\text{G}$  and  $\text{h}$  are a  $214 \times 116$  matrix and  $214 \times 1$  vector, respectively, that also vary depending on the in situ data.  $\text{G}$  and  $\text{h}$  codify a priori inequality constraints on organism and ecosystem functioning including ranges of possible gross growth efficiencies of organisms, maximum growth rates, etc. (98 constraints). An additional 116 rows in  $\text{G}$  and  $\text{h}$  (including only ones and zeroes) ensure that no ecosystem flows are negative. The mean solution of this inverse problem is achieved by first reducing the dimensionality of the problem by singular value decomposition of the matrix  $\text{E}$ . This decomposition returns a series of solutions that all satisfy the exact equations  $\text{Ex} = \text{f}$ . A set of hyperplanes bounding the solution space is then created, which contain all solutions that simultaneously satisfy  $\text{Ex} = \text{f}$  and  $\text{Gx} \geq \text{h}$ . An initial individual solution for  $\text{x}$  is chosen using the  $\text{L}_2$  minimum norm approach of Vezina and Platt (1988). We then use the constrained random walk with mirror algorithm of Van den Meersche et al. (2009) to explore the solution space, with new solutions for  $\text{x}$  chosen or rejected based on a probabilistic distribution derived from the residual errors in the approximate equalities  $\text{Ax} \approx \text{b}$ . The substantial difference in the present approach, relative to previous inverse modeling studies, is the incorporation of known and unknown  $\delta^{15}\text{N}$  values of ecosystem standing stocks into the approximate equalities  $\text{Ax} \approx \text{b}$ . Specifically, this is achieved, following Stukel et al. (2018), by making the matrix  $\text{A}$  a function of  $^{15}\text{NSS}$  where  $^{15}\text{NSS}$  is a vector of the  $^{15}\text{N}$  isotopic compositions of each of the standing stocks in the model and of upwelled  $\text{NO}_3^-$  entering the ecosystem. Since  $\delta^{15}\text{N}$  values of many of the ecosystem compartments are

not known (e.g., all the phytoplankton and protozoan taxa), we simulate  $^{15}\text{N}$ SS with a second random walk computed simultaneously. With each model step, a new solution for  $x$  and for  $^{15}\text{N}$ SS is chosen, and these new values are accepted or rejected based on the residual error of the equation:

$$A(^{15}\text{N}SS)x = b$$

These approximate equations include  $\delta^{15}\text{N}$  constraints for each of the 19 standing stocks in the model and a  $^{15}\text{N}$  mass balance constraint for the new production-export balance. The mass balance constraints and isotopic fractionation factors used to determine them can be found in the online Appendix. An additional 21 equations (of 41 total approximate equations) are related to in situ measurements: phytoplankton net production and protistan grazing losses for PRO, SYN, PEUK, DTM, AUT, and bulk phytoplankton; herbivory rates for each of the four mesozooplankton size classes and for the combined mesozooplankton community;  $\text{NO}_3^-$  uptake; sediment trap-derived sinking rates; and the relative proportion of phytoplankton and herbivory-derived fecal pellets in sinking material.

Inequality constraints in the model are mainly modified from Richardson et al. (2004) and Stukel et al. (2012). They include constraints on  $\text{NH}_4^+$  excretion and dissolved organic nitrogen (DON) production, assimilation efficiency, gross growth efficiency, maximum ingestion rates for zooplankton, and maximum phytoplankton net primary production. We assume that detritivory cannot comprise  $>50\%$  of the diets of mesozooplankton due to detritus comprising  $\sim 50\%$  of the POC in the system and the requirement of living prey for healthy mesozooplankton growth (Roman, 1984b). Active transport is constrained by assuming that excretion of  $\text{NH}_4^+$  and urea by vertically migrating taxa beneath the euphotic zone (after adjustment for temperature-dependent effects on metabolism) must be lower than excretion by those same taxa in the euphotic zone. This implicitly assumes a higher active metabolism in surface layers where these organisms are believed to feed. We set a maximum constraint on physical transport (by mixing) of DOM and suspended DET to depth by multiplying the vertical gradients of each by an eddy diffusivity constant ( $K_z$ ) of  $2 \times 10^{-4} \cdot \text{m}^2 \cdot \text{s}^{-1}$ . This  $K_z$  is derived from phytoplankton  $\text{NO}_3^-$  demand in the euphotic zone (i.e.,  $\text{NO}_3^-$  supply) and the vertical gradient of  $\text{NO}_3^-$ ; it is thus an upper-limit estimate that assumes mixing is the only source of  $\text{NO}_3^-$  to surface waters (i.e., upwelling is negligible). Additional constraint details are in the supporting information. Unless otherwise stated, values presented throughout this manuscript are mean solutions for a particular Lagrangian cycle.

#### 2.4. Comparison to the Equatorial Pacific

To compare food web structure and biogeochemistry of the CRD to the nearby open-ocean upwelling system of the equatorial Pacific, we use prior inverse modeling studies that assimilated results from the Joint Global Ocean Flux Study Equatorial Pacific Program (EqPac, Richardson et al., 2004) and the equatorial biocomplexity (EB) Program (Stukel & Landry, 2010). Because different model structures can impact results (e.g., our inclusion of planktivorous fish decreases the losses from the ecosystem attributed to mesozooplankton), we applied the data constraints from the equatorial Pacific to a model identical to the CRD model (without the  $\delta^{15}\text{N}$  component for which there were no constraints) as outlined above but with minor modifications: For the Fe-limited, high-nitrate equatorial Pacific, we assume that nitrogen fixation is negligible (inverse results also show it to be negligible in the CRD). We make this assumption because, without  $\delta^{15}\text{N}$  measurements to constrain this unmeasured rate, unrealistic solutions are possible. For the EqPac model, we also use the phytoplankton community structure of Richardson et al. (2004), as well as their published rate measurements with a few exceptions: from results presented in Décima et al. (2011), we subdivide mesozooplankton biomass and grazing into large/small and vertically migrating/surface-resident communities as was done for CRD data. Richardson et al. (2004) scaled up taxon-specific phytoplankton growth rates determined from microzooplankton grazing dilution experiments to match  $^{14}\text{C}$  net primary production measurements by multiplying by a factor of  $\sim 1.5$ . However, scaling up phytoplankton growth without scaling up protozoan grazing forced the model to an unbalanced growth-grazing condition that contradicted in situ rate measurements. We thus scaled both net primary production and grazing rates (as derived from microzooplankton dilution measurements) from the EqPac study by a constant factor to preserve the measured growth-grazing balance. We further add nitrate uptake data from Bacon et al. (1996) as a constraint on the EqPac system and use the export estimates of Dunne et al. (2000), which we believe reflect a more accurate  $\text{C}^{234}\text{Th}$  ratio than that of Bacon et al. (1996). Additional details can be found in the supporting information.

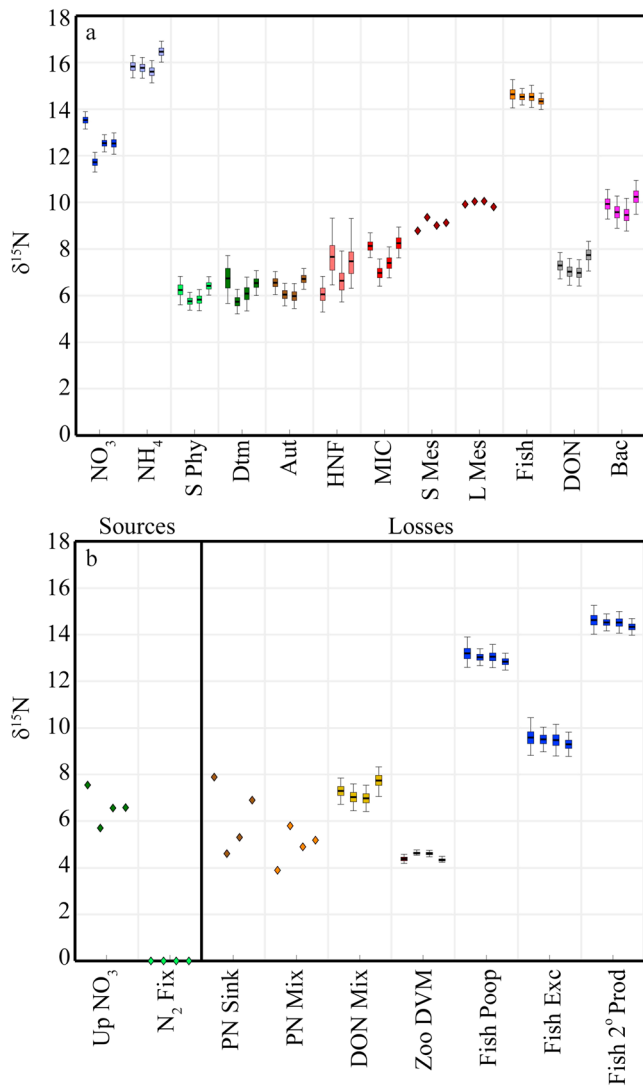


**Figure 3.** Model  $\delta^{15}\text{N}$  values. (a)  $\delta^{15}\text{N}$  for model standing stocks. (b)  $\delta^{15}\text{N}$  for fluxes of nitrogen into (left) and out of (right) the euphotic zone pelagic ecosystem. Diamonds show measured values. Whisker plots show mean, 50% confidence intervals (boxes) and 95% confidence intervals (thin lines). For each flow or compartment, whisker plots are shown for Cycles 2–5 (from left to right).

### 3. Results

#### 3.1. Model Solutions and Derived $\delta^{15}\text{N}$ Values

Mean LIEM model reconstructions do a reasonable job of reconstructing the 21 measurement relationships and 20  $\delta^{15}\text{N}$  mass balance equations that constrain the models. The normalized error ( $|(\text{A}_n x - \text{b}_n)/\sigma_{\text{b},n}|$ ) is  $<1.0$  for most measurements, and the mean of the normalized error is  $\sim 1.0$  for all cycles. We thus conclude that the LIEM model reasonably satisfies the in situ measurement constraints.

Food web structure is relatively similar across cycles (supporting information Table S1). Phytoplankton production is derived primarily from recycled  $\text{NH}_4^+$ , in agreement with in situ measurements. Large phytoplankton are responsible for most of the primary productivity (60–81% across the four cycles) as a result of higher growth rates than picophytoplankton. Protists are responsible for direct consumption of 58–65% of total phytoplankton production with the remainder going to mesozooplankton grazing (11–27%), DOM excretion (7–12%), or nongrazing mortality to detritus (8–17%). Despite the relatively small contribution of mesozooplankton to phytoplankton mortality, total ingestion by mesozooplankton is high, ranging from 12.6 to 20.0  $\text{mmol N}\cdot\text{m}^{-2}\cdot\text{day}^{-1}$ , which equates to 37–72% of their biomass consumed per day. Trophic transfer to fish is also substantial in the modeled fluxes (3.4–7.0  $\text{mmol N}\cdot\text{m}^{-2}\cdot\text{day}^{-1}$ ). Bacterial DOM uptake ranges from 6.6 to 12.3  $\text{mmol N}\cdot\text{m}^{-2}\cdot\text{day}^{-1}$ , and bacterial production is a relatively constant 11–14% of phytoplankton production. Mixotrophs are a substantial mortality term for bacteria, consuming 30–65% of bacterial production. They play a smaller but still substantial role in grazing on picophytoplankton (27–41% of grazing on cyanobacteria and PEUK). Bacteria have the largest role in  $\text{NH}_4^+$  regeneration, but protists, mesozooplankton, and fish excretion are also important sources of regenerated nutrients to the ecosystem. Detritus is rapidly recycled within the ecosystem, with only a relatively small proportion of detritus production contributing to export out of the euphotic zone.

Euphotic zone nutrient pools are significantly enriched in  $\delta^{15}\text{N}$  (11.7–13.5‰ for  $\text{NO}_3^-$  and 15.6–16.5‰ for  $\text{NH}_4^+$ ) relative to upwelled  $\text{NO}_3^-$  entering the euphotic zone (5.7–7.6‰, Figure 3a). Nevertheless, phytoplankton isotopic signatures are similar to that of the nitrate entering the ecosystem. Diatoms and picophytoplankton consistently have  $\delta^{15}\text{N}$  values between 5.7 and 6.7‰. Other eukaryotic autotrophs have marginally higher  $\delta^{15}\text{N}$  values  $\sim 6$ –7‰, reflecting the small contribution of mixotrophy to their nutritional budgets. Heterotrophic nanoflagellates,

microzooplankton, and mesozooplankton typically show gradually increasing  $\delta^{15}\text{N}$ . DOM is mildly enriched in  $^{15}\text{N}$  (7–7.7‰) relative to deep  $\text{NO}_3^-$ ; consequently, bacteria  $\delta^{15}\text{N}$  values are  $\sim 10$ ‰.

#### 3.2. Ecosystem Export Pathways

The  $\delta^{15}\text{N}$  values of nitrogen entering or leaving the euphotic zone via alternate processes provide a powerful constraint for elucidating the balance of new and export production (Figure 3b). Notably, many of the potential sources of export (DOM vertical mixing, vertically migrating fish excretion, fish fecal pellet production, and fish biomass production) have  $\delta^{15}\text{N}$  values substantially greater than either of the potential sources of nitrogen (upwelled  $\text{NO}_3^-$  or  $\text{N}_2$  fixation) to the ecosystem. Sinking detritus is also enriched in  $^{15}\text{N}$  relative to upwelled  $\text{NO}_3^-$  for two of the four cycles (and depleted by just over 1‰ for the other two cycles).

This prevalence of export sources with higher  $\delta^{15}\text{N}$  values leads to two conclusions:  $\text{N}_2$  fixation has a minimal contribution to new production in the CRD ( $\text{N}_2$  fixation  $<1\%$  of new production for all cycles; Figure 4a). In addition, the sole export mechanism with nitrogen consistently depleted in  $^{15}\text{N}$  relative to deep  $\text{NO}_3^-$

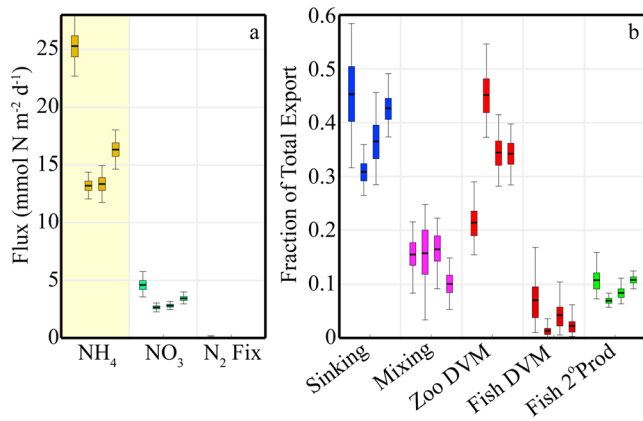


**Figure 4.** Export-new production balance. (a) Nitrogen sources to the phytoplankton community. (b) Fraction of total export driven by different processes (sinking includes sinking detritus and fish fecal pellets, mixing included POM and DOM, DVM includes excretion of DOM and NH<sub>4</sub><sup>+</sup> beneath the euphotic zone). Whisker plots show mean, 50% confidence intervals (boxes) and 95% confidence intervals (thin lines). For each flux, whisker plots are shown for Cycles 2–5 (from left to right). DOM = dissolved organic matter; POM = particulate organic matter.

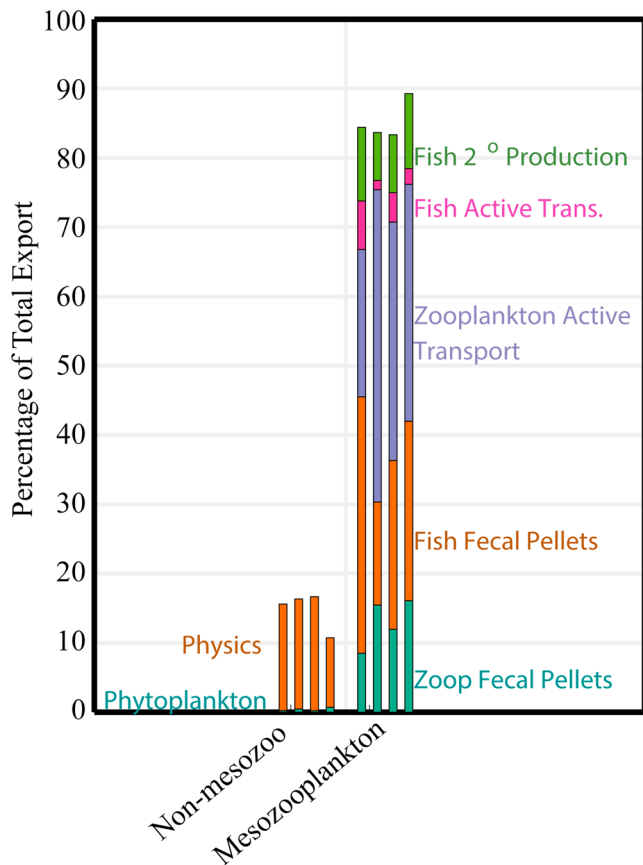


**Figure 5.** Euphotic zone export of carbon that was not consumed by mesozooplankton (left) and export of carbon that was consumed by mesozooplankton (right). Bar plots are shown for Cycles 2–5 (from left to right).

(excretion at depth by vertically migrating mesozooplankton,  $\delta^{15}\text{N}$  value of 4.3–4.7, Figure 3b) must play a substantial role in export flux (Figure 4b). Zooplankton active transport (excretion of DOM and NH<sub>4</sub><sup>+</sup>) is responsible for 21–45% of total export from the euphotic zone. Sinking organic matter (including sinking detritus collected by sediment trap and rapidly sinking fish fecal pellets) contributes a similar fraction of export (31–46%), while vertical mixing of POM and DOM accounts for less (10–16%). The lowest contributions to export are from fish biomass production (7–11%) and fish active transport (1–7%).

The above results make clear the central importance of mesozooplankton in vertical transport of POM from the euphotic zone of the CRD. Mesozooplankton active transport is a dominant vertical transport mechanism, and only 11–17% of export is not mediated at least indirectly by mesozooplankton (Figure 5). Nonmesozooplankton mediated export is predominantly driven by physical mixing, with sinking phytoplankton responsible for <1% of export. The relative contributions of mesozooplankton and fish fecal pellets to export vary from roughly equal to a substantially greater importance of fish fecal pellets. Nonetheless, mesozooplankton fecal pellet production always exceeds that by fish. The relatively higher importance of fish fecal pellets in sinking derives from high remineralization rates of mesozooplankton fecal pellets in the euphotic zone (loss terms including microbial degradation, dissolution to DOM, and consumption by mesozooplankton). Substantial remineralization of mesozooplankton fecal pellets within the euphotic zone is also supported by in situ data, which show that phaeopigment flux into sediment traps accounts for only a small fraction of the phaeopigments produced by mesozooplankton grazing (Décima et al., 2016; Stukel, Décima, et al., 2013).

### 3.3. Mesozooplankton Dynamics

Given the dominant role of mesozooplankton in the euphotic zone nitrogen budget and their importance in supporting a large biomass of higher trophic consumers in the CRD, a more detailed examination of mesozooplankton growth dynamics is warranted. Our a priori expectation was that high rates of mesozooplankton secondary production in a picophytoplankton-dominated ecosystem would require efficient mesozooplankton growth. To the contrary, the results suggest modest gross growth efficiencies for mesozooplankton, with cycle averages ranging from 16 to 28% for the different mesozooplankton classes, although there is substantial uncertainty in the gross growth efficiency of the small size fraction (Figure 6b). As expected, protists have higher gross growth efficiencies (typically >30%), which facilitate efficient transfer of picoplanktonic production to mesozooplankton. Consequently, protistan grazers are the major food source for mesozooplankton, contributing 32–53% of their diet (Figure 6a). With the exception of Cycle 5, this pathway supplies more than twice the prey biomass flux as herbivory, which contributes 16–32% of mesozooplankton nitrogen. Detritivory also emerges as an important feeding mode for mesozooplankton (11–40% of diet), while carnivory (predation on metazoans) accounts for only 7–15% of mesozooplankton community diet and 15–34% of the ingestion of larger (>1 mm) mesozooplankton.

The importance of detritivory in mesozooplankton diets is a robust result of the LIEM. At the 95% confidence interval, detritivory exceeds 24% of mesozooplankton diets for Cycles 3 and 4 and exceeds 15% for Cycle 5.

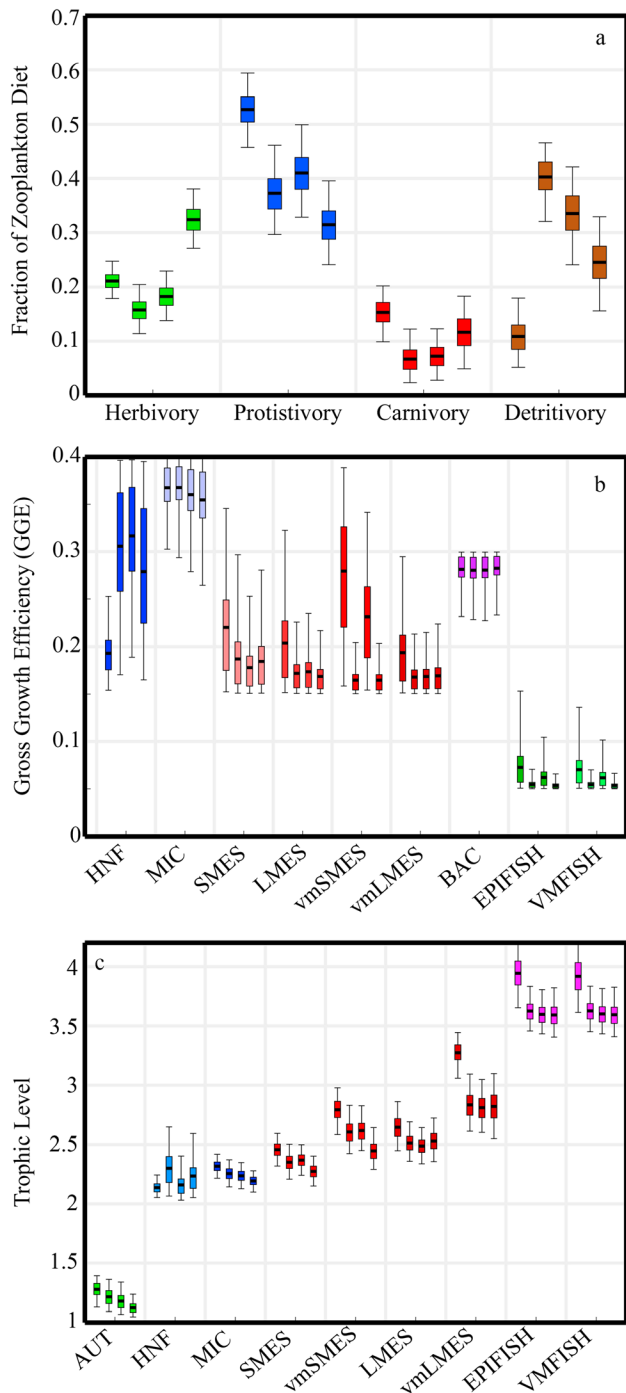


**Figure 6.** Zooplankton prey and growth. (a) Proportion of different food sources in mesozooplankton diets. (b) Gross growth efficiencies of model heterotrophs. (c) Trophic levels of mixotrophs and consumers (TL = 1 assumed for autotrophs and TL = 2 for heterotrophic bacteria). Whisker plots show mean, 50% confidence intervals (boxes) and 95% confidence intervals (thin lines). For each ecosystem flow or compartment, whisker plots are shown for Cycles 2–5 (from left to right). HNF = heterotrophic nanoflagellates; MIC = microzooplankton; SMES = small (<1-mm) nonvertically migrating mesozooplankton; VMSMES = small vertically migrating mesozooplankton; LMES = large nonvertically migrating mesozooplankton; VMLMES = large vertically migrating mesozooplankton; EPIFISH = epipelagic fish; VMFISH = vertically migrating fish; BAC = bacteria.

It was only for Cycle 2 that the LIEM allows detritivory to comprise <15% of the diet; yet the mean contribution is 11% (with 95% confidence intervals of 5–18%) even for this cycle. Although detritivory is not easily demonstrated in field studies, several independent pieces of evidence support its importance in the CRD. First, the sum of the biomasses of autotrophic and heterotrophic nanoplankton and microplankton comprises only 16–30% of the POM in the euphotic zone (Freibott et al., 2016; Stukel et al., 2016; Taylor et al., 2016). Second, the phaeopigment:Chl *a* ratio, a tracer of zooplankton degradation of Chl *a*, is unusually high in the water column in the CRD, and the ratio of phaeopigment production by zooplankton to export flux at 90-m depth is low. Third, phycoerythrin (a diagnostic pigment for SYN) measured in the guts of mesozooplankton is consistent with feeding on SYN contained in >20- $\mu$ m aggregates (Décima et al., 2016; Stukel, Décima, et al., 2013).

Trophic levels (TL) are calculated assuming that obligate phototrophs are TL = 1 and bacteria are TL = 2. Detritus  *trophic level* is calculated based on the proportion of phytoplankton or fecal pellets contributing to the detritus and the assumption that fecal pellets have TLs one less than the organism producing them (e.g., an herbivorous protist produces egesta with TL = 1 reflecting the TL of its prey). Mesozooplankton TLs typically vary between two and three, reflecting an omnivorous diet on phytoplankton and protistan energy sources. Small mesozooplankton (<1 mm) are only slightly enriched relative to protists, which have mean TLs of 2.1–2.3 since some of their nutrition derives from heterotrophic bacteria. TLs increase with increasing mesozooplankton size and are also higher on average for vertical migrators than for euphotic zone-resident mesozooplankton. For large migrants, TL estimates are ~2.8 for Cycles 3–5 but exceed 3 for Cycle 2. Mixotrophs have consistently lower TLs (1.1–1.3) reflecting dissolved nutrients as their main source of N.

Mesozooplankton excrete 21–31% of the nitrogen consumed as  $\text{NH}_4^+$  and an additional 11–16% as DOM. This highlights the important, yet often overlooked, role of mesozooplankton in nutrient regeneration. Altogether, 15–20% of mesozooplankton excretion occurs at depth, with the remainder in the euphotic zone. Taking into account that only 12–23% of mesozooplankton fecal pellet nitrogen is exported from the euphotic zone, it becomes clear that mesozooplankton contribute substantially to nutrient-regeneration food webs in the CRD.

### 3.4. Comparison of CRD and Equatorial Pacific

To compare food webs in the CRD and equatorial Pacific upwelling biomes, we computed LIEM solutions assimilating data from the EB project and the Joint Global Ocean Flux Study (JGOFS) Equatorial Pacific (EqPac) time series cruises. These results simultaneously demonstrate that our results in the CRD are not determined by choice of model structure and highlight key ways in which the CRD differs from the equatorial Pacific (Figure 7). Model primary productivity and *f* ratios are broadly similar between the regions (although EB primary productivity was lower than CRD or EqPac), as suggested by the input data (Figures 1 and 7a). Although similarities in *f* ratios imply that similar fractions of primary production are recycled, the organisms responsible for regenerating  $\text{NH}_4^+$  differ between the regions. In the CRD,  $\text{NH}_4^+$  production is derived nearly equally from heterotrophic bacteria, protists, and metazoans (fish + mesozooplankton). In the equatorial Pacific, heterotrophic bacteria play a much

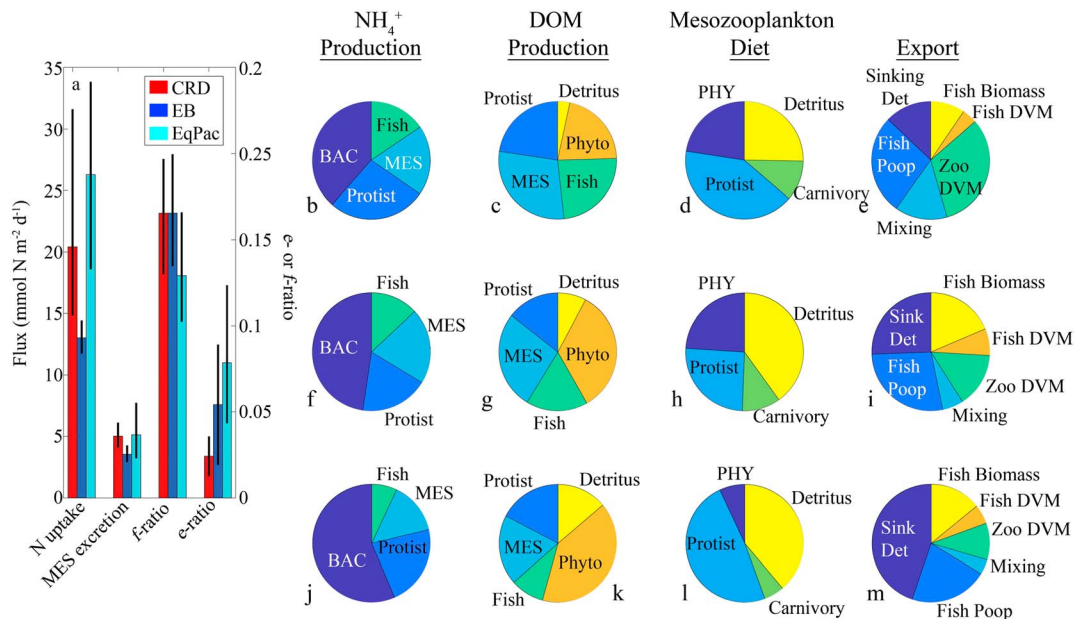


**Figure 7.** Comparison of CRD to equatorial Pacific. Bar chart compares model results for total N uptake, mesozooplankton excretion ( $\text{NH}_4^+$  and DOM),  $f$  ratio (new production/net primary production), and  $e$  ratio (sinking detritus export/net primary production) with 95% confidence intervals (a). Pie charts show organisms responsible for  $\text{NH}_4^+$  regeneration (b, f, j) and DOM production (c, g, k), mesozooplankton dietary sources (d, h, l), and the processes responsible for export (e, i, m). Figures 7b–7e are CRD data (combined for all four cycles). Figures 7f–7m show results of equatorial Pacific LIM models assimilating data from the equatorial biocomplexity cruises (Figures 7f–7i) and the EqPac time series cruises (Figures 7j–7m). CRD = Costa Rica Dome; DOM = dissolved organic matter; BAC = bacteria; EB = equatorial biocomplexity; EqPac = equatorial Pacific.

more substantial role in nutrient cycling, accounting for just under half and  $>50\%$  of  $\text{NH}_4^+$  production in the EB and EqPac models, respectively (Figures 7b, 7f, and 7j). The source of DOM supporting bacterial production also varies substantially between the regions, with zooplankton and fish responsible for  $>75\%$  of DOM production in the CRD, while phytoplankton and detritus breakdown play a much greater proportional role in the equatorial Pacific (Figures 7c, 7g, and 7k).

Despite similar or slightly lower  $f$  ratios in the equatorial Pacific, the  $e$  ratio (sinking detritus/net primary productivity) is substantially greater in the equatorial Pacific studies than in the CRD. This reflects a greater proportional importance of sinking detritus (and mesozooplankton fecal pellets, specifically) to total export in the equatorial Pacific. In the CRD, gravitational settling of particles (including sinking detritus and fish fecal pellets) comprise approximately one third of total export, while in both equatorial Pacific studies gravitational settling contributes greater than one-half of export. The other significant difference between regions is the substantially more important role of active transport by diel vertically migrating mesozooplankton in the CRD (32% of export) than in the equatorial Pacific (15% for EB; 10% for EqPac).

## 4. Discussion

### 4.1. Food Web Organization and LIEM Considerations

The MCMC approach allows us to quantify explicitly the model output uncertainties arising from two key sources: model underdeterminacy and uncertainty in input parameters (Kones et al., 2009, 2006). However, these model values and uncertainty estimates are sensitive to a priori decisions made about model structure (i.e., what food web compartments should be included and how should they be connected) and about what inequality constraints should be used. For instance, based on results in Straille (1997) we constrained gross growth efficiency for all zooplankton groups to 15–40%, although other ranges (e.g., 10–45%) could also have been defensible. Such modifications can affect the model mean and uncertainty estimates, although MCMC method solutions are less sensitive to the bounds of the inequality constraints than  $L_2$  minimum norm solutions (Stukel et al., 2012). We found that our model was sensitive to the lower limits of excretion chosen for protists, the upper limits for microzooplankton and bacterial gross growth efficiency, and the lower limits for zooplankton and fish gross growth efficiency. To test the sensitivity of the model to inequality constraints, we

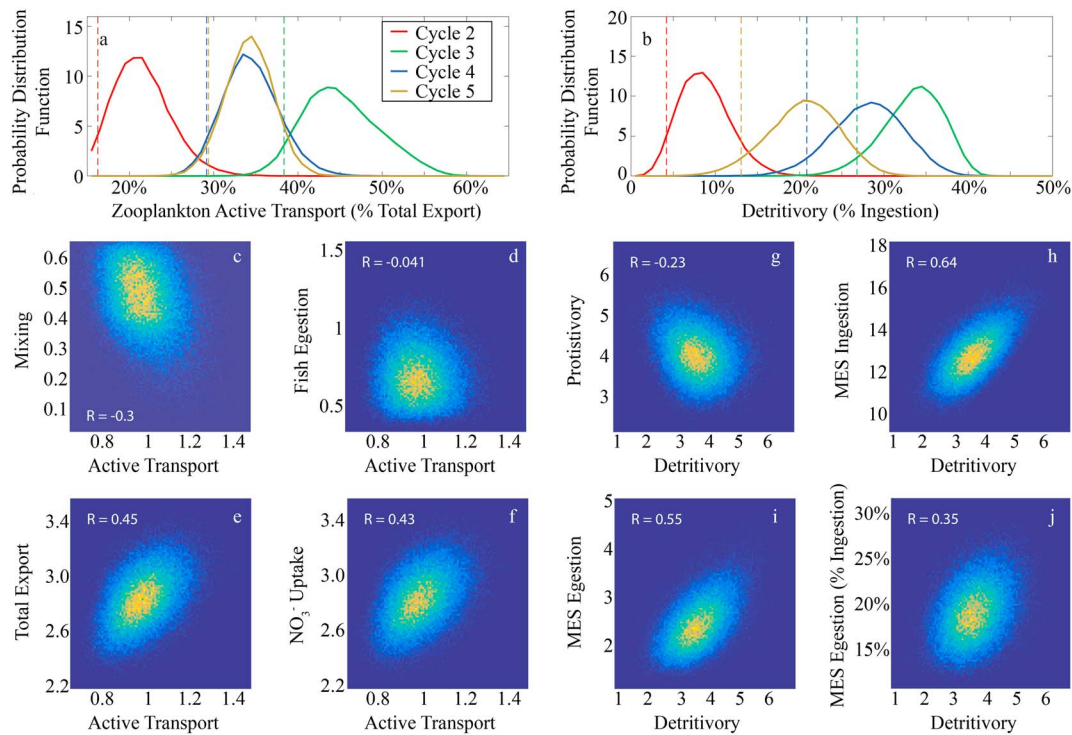


**Figure 8.** Variability in active transport by diel vertically migrating mesozooplankton (a and c–f) and mesozooplankton detritivity (b and g–j). Probability distribution functions of zooplankton active transport (Figure 8a) and detritivity (Figure 8b) from the LIEM solution vectors. Vertical dashed lines show one-sided 95% confidence intervals (lower bounds on the values for each cycle). Lower panels are heat maps of property-property plots for LIEM solution vectors showing relationship between active transport (c–f) or detritivity (g–j) and other ecosystem rates. Figures 8c–8h have units of  $\text{mmol N}\cdot\text{m}^{-2}\cdot\text{day}^{-1}$ . In Figure 8j, y axis is percentage of ingested nitrogen that is egested as fecal pellets. Figures 8c–8j are for Cycle 4 (which had typical rates of active transport and detritivity) only. All  $p$  values were  $<<10^{-4}$ . LIEM = linear inverse ecosystem modeling.

ran a model simulation with gross growth efficiency bounds increased to 10–45%. In this simulation, most model flows were modified by  $<4\%$  (the median of the absolute value of percent change was 3.2%). The largest percentage change of any model flux was a 21.6% increase in the egestion of large, nonvertically migrating mesozooplankton, although this was still a relatively small change in absolute magnitude of the flux (from 0.63 to 0.77  $\text{mmol N}\cdot\text{m}^{-2}\cdot\text{day}^{-1}$ ). By contrast, the model was relatively insensitive to other inequalities (e.g., assimilation efficiency). The model is likely also sensitive to the isotopic fractionation factors for  $^{15}\text{N}$ . These values were assumed from prior knowledge (Appendix 2; Altabet, 2001; Altabet & Francois, 2001; Altabet et al., 1999; Altabet & Small, 1990; Calleja et al., 2013; Checkley & Entzeroth, 1985; Checkley & Miller, 1989; Cifuentes et al., 1989; De Brabandere et al., 2007; Décima et al., 2017; Gutierrez-Rodriguez et al., 2014; Hoch et al., 1996; Horrigan et al., 1990; Landry & Décima, 2017; Mayor et al., 2011; Mino et al., 2016; Möbius, 2013; Montoya et al., 1991; Montoya & McCarthy, 1995; Needoba et al., 2003; Pennock et al., 1996; Sigman et al., 1999; Steffan et al., 2015; Tamelander et al., 2006; Voss et al., 1997; Waser et al., 1998; Wu et al., 1997) but are likely variable in situ. Further development of the MCMC +  $^{15}\text{N}$  approach to incorporate uncertainties in these parameters may lead to wider uncertainty estimates on some modeled rates.

Despite these caveats, by combining extensive in situ ecosystem rate measurements with isotopic signature constraints for key components of the ecosystem, the MCMC +  $^{15}\text{N}$  approach allowed us to determine robust estimates of food web structure with associated uncertainties. These uncertainty estimates, however, are still substantial for many of the food web flows (supporting information Table S1). We thus consider below the uncertainties associated with two key conclusions from this study: the large role of diel vertical migration in export flux and the important contribution of detritus to mesozooplankton diets.

Each of our cycle experiments can be considered an independent ecosystem realization—a snapshot capturing one possible configuration of stocks and rates during the evolution of the water parcel sampled. For each

of these realizations, the MCMC+<sup>15</sup>N approach also generates tens of thousands of solution vectors that are consistent with the in situ measurements and a priori knowledge of pelagic ecosystem structure and organismal capability. By querying the variability among these solution vectors, we can gain insight into the likelihood of different food web pathways beyond the mean values reported. A histogram of the percentage contribution of mesozooplankton active transport to total export shows that active transport was >25% of total export for Cycles 3–5 (one-sided 95% confidence interval, Figure 8a) and >38% for Cycle 3. For Cycle 3, specifically, the available data suggest that active transport more likely exceeded 50% of total export than was less than 38% of export. These substantial contributions are derived from (1) the large abundance of vertical migrants, (2) the high efficiency of protistan secondary production in transferring picoplankton C and N productivity to mesozooplankton, and (3) the ability of the zooplankton community to utilize and recycle fecal pellets and detritus that would otherwise remove nitrogen as sinking export from the ecosystem.

To further assess the food web constraints that lead to high mesozooplankton active transport, we look at correlations among food web flows using the independent MCMC solution vectors, focusing on Cycle 4, which was typical with respect to both active transport and detritivory. We find strong positive correlations between mesozooplankton active transport and both total export and total NO<sub>3</sub> uptake ( $R = 0.45$  and  $0.43$ , respectively). Negative correlations also occur for most of the other processes responsible for export ( $R = -0.30$  for mixing;  $R = -0.087$  for sinking particles; and  $R = -0.041$  for fish fecal pellet production), suggesting that migrant-mediated flux is the most likely pathway for the model to export sufficient nitrogen to balance the measured nitrate uptake. There is, however, a positive correlation between zooplankton active transport and fish biomass production ( $R = 0.24$ ), which likely arises as a result of positive correlations between zooplankton secondary production and both fish production and active transport.

In the model, predation by planktivorous fish is the only loss term for the secondary production of >1-mm mesozooplankton. This, of course, oversimplifies the complex higher-level food web with predators including cetaceans, seabirds, ctenophores, and cnidarians. Furthermore, rapid sinking of uneaten carcasses can be a significant loss term for mesozooplankton (Elliott et al., 2010; Frangoulis et al., 2011; Smith et al., 2014). Therefore, the export terms derived from mesozooplankton secondary production (fish fecal pellets, fish biomass production, and active transport by vertically migrating fish) collectively represent the export processes associated with rare large particles, secondary production, and nitrogen removal by higher trophic levels.

The histogram of percentage detritivory in mesozooplankton diets shows greater uncertainty than for active transport. Mean percentage contributions of detritivory in mesozooplankton diets are 9%, 33%, 28%, and 21% for Cycles 2–5, respectively. One-sided 95% confidence limits suggest that detritivory accounts for at least 4%, 27%, 21%, and 13% of mesozooplankton diets for Cycles 2–5. If the model required substantial detritivory to meet mesozooplankton metabolic requirements, we would expect to see strongly negative correlations between zooplankton ingestion of detritus and other food sources. However, the correlation between detritivory and protistivory is weak ( $R = -0.23$ , Figure 8g), and correlations between detritivory and herbivory or carnivory are positive ( $R = 0.066$  and  $0.14$ , respectively). A much stronger correlation occurs between detritivory and total ingestion rate ( $0.64$ , Figure 8h). This suggests that high detritivory in model solutions was not required to satisfy mesozooplankton consumption demand but served instead to balance high detritus production. Indeed, we find a strong correlation between mesozooplankton egestion and detritivory ( $R = 0.55$ , Figure 8i), with high detritivory supported despite modest egestion rates (~20% of ingestion, Figure 8j). Substantial mesozooplankton consumption of fecal pellets is a sensible conclusion, given the high mesozooplankton abundances and relative paucity of fecal pellet signatures from herbivory in sediment trap samples (Décima et al., 2016; Stukel, Décima, et al., 2013).

Although few field studies have quantified zooplankton detritivory, our conclusion of its importance is not unprecedented. Mesozooplankton feeding on detritus, aggregates, and fecal pellets has been detected in many environments (Dilling & Brzezinski, 2004; Paffenhöfer & Strickland, 1970; Park et al., 2011; Roman, 1984a; Roman & Tenore, 1984; Wilson et al., 2010) and laboratory studies (Dilling et al., 1998; Paffenhöfer & Strickland, 1970; Roman, 1984b). Although detritus feeding is difficult to detect from gut content analyses, transmission electron microscopy has identified detritivory as a dominant nutritional mode in benthopelagic copepods from the coastal northeast Pacific (Gowing & Wishner, 1986). Detritivory has also been identified through incorporation of <sup>3</sup>H-labeled bacteria in surface layers of the Gulf Stream and Sargasso Sea (Roman, 1984a). Further, in the subtropical and subpolar North Pacific, mesozooplankton fatty acid

signatures representative of heterotrophic bacteria and picophytoplankton have been detected in mesozooplankton guts and interpreted as evidence of zooplankton feeding on aggregates (Wilson et al., 2010; Wilson & Steinberg, 2010).

The processes leading to efficient retention of mesozooplankton fecal pellets in the euphotic zone cannot be determined from this study, but possible hypotheses include a strong density gradient that retards sinking speeds, low sinking rates resulting from the paucity of biogenic silica ballast (Krause et al., 2016), the relatively low proportion of taxa (e.g., salps and euphausiids) known to produce rapidly sinking fecal pellets (Décima et al., 2016), and deep euphotic zone communities specializing in flux feeding. As key players in nitrogen regeneration pathways in the CRD, mesozooplankton facilitate nitrogen recycling and increase the efficiency of secondary production and energy transfer to abundant populations of seabirds, cetaceans, and fish (Reilly & Thayer, 1990; Vilchis et al., 2006).

#### 4.2. New Production, Export, and Mesozooplankton Secondary Production

Mass balance requires that the amount of nitrogen entering the planktonic ecosystem be offset by the amount of nitrogen exported (Eppley & Peterson, 1979). Although it was originally assumed that sinking particle flux would balance nitrogen entering the euphotic zone through upwelling of nitrate and  $N_2$  fixation, evidence from multiple ecosystems suggests that other processes must serve as nitrogen export terms. In the Sargasso Sea, for example, 2 years of nitrate uptake measurements have shown a substantially higher  $f$  ratio (0.08–0.39) than the  $e$  ratio measured by sediment traps (0.04–0.06 for the same years, Lipschultz, 2001; Lomas et al., 2013), and net community production (functionally similar to new production) has been found to exceed  $^{238}\text{U}$ : $^{234}\text{Th}$ -derived export on average (Estepa et al., 2015). Similarly, JGOFS studies in the equatorial Pacific and Arabian Sea have pointed to excess new production relative to export (Buesseler et al., 1995, 1998; McCarthy et al., 1996; Sambrotto, 2001). In the western Antarctic Peninsula, twice weekly sampling has demonstrated that both nitrate uptake and net community production substantially exceed export from sediment trap and  $^{238}\text{U}$ : $^{234}\text{Th}$  disequilibrium measurements when integrated over the phytoplankton growing season, and regional cruises have reported similar production-export imbalances (Ducklow et al., 2018; Stukel et al., 2015). Similar imbalances have also been noted between the flux of sinking carbon out of the euphotic zone and the carbon demand of mesopelagic communities below (Burd et al., 2010).

These results imply that other processes beyond gravitational particle sinking are quantitatively important in removing nitrogen from the euphotic zone. Steinberg et al. (2008) suggested that high migrant-mediated active transport is necessary to meet the carbon demand of mesopelagic bacteria and zooplankton in the subtropical and subpolar Pacific. Carlson et al. (1994) determined that DOC transport by vertical mixing exceeds sinking carbon flux in the Sargasso Sea. Similarly, Levy et al. (2013) used a biogeochemical model to show that subduction of POC may be an important export term, and Stukel and Ducklow (2017) found that vertical mixing of POC could account for 20–50% of the biological pump in the Southern Ocean. Davison et al. (2013) further concluded that export by myctophid fish comprised >15% of the total export in the California Current Ecosystem.

Based on the extensive stock and process measurements and stable isotope constraints from our CRD cruise, our model indicates that sinking particles (including fish fecal pellets) and active transport by diel vertically migrating mesozooplankton each comprise roughly one third of total export. The remaining export comes about equally from vertical mixing of POM and DOM and the combined biomass production and active transport of higher trophic levels.

Using conservative assumptions and data from a range of sites, Longhurst et al. (1990) estimated that migrant-mediated transport is typically 5–20% of carbon flux from sinking particles. Bianchi et al. (2013) estimated that active transport was globally equivalent to 15–40% of sinking particle flux. In regions closer to our study site, active transport at station ALOHA in the subtropical Pacific is ~20% of sediment trap-measured carbon export and ~40% of sediment trap-measured nitrogen export (Hannides et al., 2009), and active transport in the California Current Ecosystem ranges from 1.9 to 40.5% of sinking carbon flux with a greater contribution in coastal, high-biomass locations (Stukel, Ohman, et al., 2013). In the equatorial Pacific, Zhang and Dam (1997) gave active transport rates ranging from 31 to 44% of sinking carbon flux, and Hidaka et al. (2001) estimated that zooplankton migrants accounted for 18–43% of sinking carbon, with

micronekton contributing an additional 28–55%. Le Borgne and Rodier (1997) found higher proportional contributions of zooplankton and micronekton in the western equatorial Pacific (40% of sinking nitrogen) than in the eastern equatorial Pacific (9% of sinking nitrogen). For comparison, our equatorial Pacific models indicate that zooplankton active transport is responsible for 23% of sinking nitrogen flux (excluding fish fecal pellets) from EqPac data and 59% from EB data. Based on these comparisons, our estimates of zooplankton-mediated active fluxes equivalent to passive export in the CRD are on the higher end of previous studies. They are not unreasonable, however, given that most studies exclude processes like excretion, egestion, or mortality at depth or migratory complexities (foraging sorties and reverse diel migrations) that would broadly be folded into our constrained model balances. Furthermore, our study uses nitrogen currency, while the previous studies were carbon centric, which can lead to slight differences if nitrogen is preferentially remineralized in sinking particles or metabolized differently by zooplankton. In addition, our results also reflect the somewhat unique ecological conditions of the CRD that lead to high mesozooplankton biomasses coupled with relatively low export ratios measured by sediment traps.

Across the four cycles, total mesozooplankton community ingestion ranged from 1.5% to 3.0% of total biomass  $\text{h}^{-1}$ . For comparison, based on the temperature- and allometric-scaling relationships in Hansen et al. (1997), maximum potential ingestion rates for CRD mesozooplankton might be as high as 12% of total biomass  $\text{h}^{-1}$ . Mesozooplankton excrete 33–48% of the ingested nitrogen as  $\text{NH}_4^+$  or DOM, with 27–29% of vertical migrant excretion occurring below the euphotic zone and 15–20% of the excretion of the entire mesozooplankton community occurring at depth. We find no reason to suspect that these model outputs are unrealistic and hence conclude that active transport is a particularly important export process in the CRD. However, large uncertainty estimates (Figure 4) do indicate that the contribution of active transport may be as low as 15% on Cycle 2 and as high as 55% on Cycle 3. Furthermore, our results do not preclude the possibility that nonlinear dynamics may lead to increased export due to subduction or sinking particles at mesoscale and submesoscale features (Omand et al., 2015; Stukel et al., 2017).

## 5. Conclusions

The central role of mesozooplankton in the biogeochemistry of the CRD is a robust conclusion of our ecosystem inverse model. Despite large biomasses of picophytoplankton, particularly cyanobacteria, and the dominance of protists as grazers on phytoplankton, mesozooplankton are able to meet their metabolic requirements by obtaining substantial supplementary nutrition through protistivory and detritivory. While important questions remain regarding the specific processes that promote fecal pellet retention (e.g., slow sinking rates, high bacterial consumption, and/or widespread zooplankton coprophagy) we find that fecal pellets are primarily utilized and remineralized within the euphotic zone. As a result, mesozooplankton are more important to organic recycling in the CRD ecosystem than in the nearby equatorial Pacific or likely most systems generally. This recycling also contributes to efficient energy transfer to higher trophic levels. Ingestion of protists, detritus, and phytoplankton in surface layers by diel vertically migrating mesozooplankton also contributes substantially to the biological pump. These results underscore the essential role that zooplankton can play in carbon cycling and trophic processes in open-ocean ecosystems, despite the dominance of picophytoplankton, and suggest that simple paradigms relating these processes to phytoplankton size structure need to be reevaluated.

## References

- Altabet, M. A. (2001). Nitrogen isotopic evidence for micronutrient control of fractional  $\text{NO}_3^-$  utilization in the equatorial Pacific. *Limnology and Oceanography*, 46(2), 368–380. <https://doi.org/10.4319/lo.2001.46.2.0368>
- Altabet, M. A., & Francois, R. (2001). Nitrogen isotope biogeochemistry of the Antarctic polar frontal zone at 170 degrees W. *Deep-Sea Research Part II*, 48(19–20), 4247–4273. [https://doi.org/10.1016/S0967-0645\(01\)00088-1](https://doi.org/10.1016/S0967-0645(01)00088-1)
- Altabet, M. A., Pilskaln, C., Thunell, R., Pride, C., Sigman, D., Chavez, F., & Francois, R. (1999). The nitrogen isotope biogeochemistry of sinking particles from the margin of the eastern North Pacific. *Deep-Sea Research Part I*, 46(4), 655–679. [https://doi.org/10.1016/S0967-0637\(98\)00084-3](https://doi.org/10.1016/S0967-0637(98)00084-3)
- Altabet, M. A., & Small, L. F. (1990). Nitrogen isotopic ratios in fecal pellets produced by marine zooplankton. *Geochimica et Cosmochimica Acta*, 54(1), 155–163. [https://doi.org/10.1016/0016-7037\(90\)90203-W](https://doi.org/10.1016/0016-7037(90)90203-W)
- Bacon, M. P., Cochran, J. K., Hirschberg, D., Hammar, T. R., & Fleer, A. P. (1996). Export flux of carbon at the equator during the EqPac time-series cruises estimated from Th-234 measurements. *Deep-Sea Research Part II*, 43(4–6), 1133–1153. [https://doi.org/10.1016/0967-0645\(96\)00016-1](https://doi.org/10.1016/0967-0645(96)00016-1)

### Acknowledgments

We are deeply indebted to the Captain and crew of the R.V. *Melville* and to many of our colleagues from the CRD FluZiE project. We also thank Tom Kelly for assistance with coding. The code used in this manuscript (and an example setup file) can be downloaded from GitHub at <https://github.com/stukel-lab/N15-LIM>. A version of the code specific to this manuscript is available with the online supporting information. The in situ data assimilated by the model is available on BCO-DMO and in Table 1. Model results are available in online supporting information Table S1. This paper is a result of research supported by the National Oceanic and Atmospheric Administration's RESTORE Science Program under federal funding opportunity NOAA-NOS-NCCOS-2017-2004875 and U. S. National Science Foundation (NSF) grant OCE-1756610 to M. Stukel, U. S. NSF grants OCE-0826626 and OCE-1260055 to M. Landry, and NIWA award CDPD 1601 to M. Décima.

- Balch, W., Poulton, A., Drapeau, D., Bowler, B., Windecker, L., & Booth, E. (2011). Zonal and meridional patterns of phytoplankton biomass and carbon fixation in the equatorial Pacific Ocean, between 110 W and 140 W. *Deep Sea Research, Part II*, 58(3-4), 400–416. <https://doi.org/10.1016/j.dsr2.2010.08.004>
- Barber, R. T., Sanderson, M. P., Lindley, S. T., Chai, F., Newton, J., Trees, C. C., et al. (1996). Primary productivity and its regulation in the equatorial Pacific during and following the 1991–1992 El Niño. *Deep-Sea Research Part II*, 43(4–6), 933–969. [https://doi.org/10.1016/0967-0645\(96\)00035-5](https://doi.org/10.1016/0967-0645(96)00035-5)
- Bianchi, D., Stock, C., Galbraith, E. D., & Sarmiento, J. L. (2013). Diel vertical migration: Ecological controls and impacts on the biological pump in a one-dimensional ocean model. *Global Biogeochemical Cycles*, 27, 478–491. <https://doi.org/10.1002/gbc.20031>
- Buchwald, C., Santoro, A. E., Stanley, R. H. R., & Casciotti, K. L. (2015). Nitrogen cycling in the secondary nitrite maximum of the eastern tropical North Pacific off Costa Rica. *Global Biogeochemical Cycles*, 29, 2061–2081. <https://doi.org/10.1002/2015GB005187>
- Buesseler, K., Ball, L., Andrews, J., Benitez-Nelson, C., Belostock, R., Chai, F., & Chao, Y. (1998). Upper ocean export of particulate organic carbon in the Arabian Sea derived from thorium-234. *Deep-Sea Research Part II*, 45(10–11), 2461–2487. [https://doi.org/10.1016/S0967-0645\(98\)80022-2](https://doi.org/10.1016/S0967-0645(98)80022-2)
- Buesseler, K. O., Andrews, J. A., Hartman, M. C., Belostock, R., & Chai, F. (1995). Regional estimates of the export flux of particulate organic carbon derived from thorium-234 during the JGOFS EqPac program. *Deep-Sea Research Part II*, 42(2–3), 777–804. [https://doi.org/10.1016/0967-0645\(95\)00043-P](https://doi.org/10.1016/0967-0645(95)00043-P)
- Burd, A. B., Hansell, D. A., Steinberg, D. K., Anderson, T. R., Aristegui, J., Baltar, F., et al. (2010). Assessing the apparent imbalance between geochemical and biochemical indicators of meso- and bathypelagic biological activity: What the @#! is wrong with present calculations of carbon budgets? *Deep-Sea Research Part II*, 57(16), 1557–1571. <https://doi.org/10.1016/j.dsr2.2010.02.022>
- Calleja, M. L., Batista, F., Peacock, M., Kudela, R., & McCarthy, M. D. (2013). Changes in compound specific  $\delta^{15}\text{N}$  amino acid signatures and d/l ratios in marine dissolved organic matter induced by heterotrophic bacterial reworking. *Marine Chemistry*, 149(Supplement C), 32–44. <https://doi.org/10.1016/j.marchem.2012.12.001>
- Carlson, C. A., Ducklow, H. W., & Michaels, A. F. (1994). Annual flux of dissolved organic carbon from the euphotic zone in the northwestern Sargasso Sea. *Nature*, 371(6496), 405–408. <https://doi.org/10.1038/371405a0>
- Casciotti, K. L. (2016). Nitrogen and oxygen isotopic studies of the marine nitrogen cycle. *Annual Review of Marine Science*, 8(1), 379–407. <https://doi.org/10.1146/annurev-marine-010213-135052>
- Checkley, D. M., & Entzeroth, L. C. (1985). Elemental and isotopic fractionation of carbon and nitrogen by marine, planktonic copepods and implications to the marine nitrogen cycle. *Journal of Plankton Research*, 7(4), 553–568. <https://doi.org/10.1093/plankt/7.4.553>
- Checkley, D. M., & Miller, C. A. (1989). Nitrogen isotope fractionation by oceanic zooplankton. *Deep-Sea Research*, 36(10), 1449–1456. [https://doi.org/10.1016/0198-0149\(89\)90050-2](https://doi.org/10.1016/0198-0149(89)90050-2)
- Childress, J. J., Taylor, S. M., Cailliet, G. M., & Price, M. H. (1980). Patterns of growth, energy utilization and reproduction in some meso- and bathypelagic fishes off Southern California. *Marine Biology*, 61(1), 27–40. <https://doi.org/10.1007/BF00410339>
- Cifuentes, L. A., Fogel, M. L., Pennock, J. R., & Sharp, J. H. (1989). Biogeochemical factors that influence the stable nitrogen isotope ratio of dissolved ammonium in the Delaware estuary. *Geochimica et Cosmochimica Acta*, 53(10), 2713–2721. [https://doi.org/10.1016/0016-7037\(89\)90142-7](https://doi.org/10.1016/0016-7037(89)90142-7)
- Conover, R. J. (1966). Assimilation of organic matter by zooplankton. *Limnology and Oceanography*, 11(3), 338–345. <https://doi.org/10.4319/lo.1966.11.3.0338>
- Dam, H. G., Zhang, X. S., Butler, M., & Roman, M. R. (1995). Mesozooplankton grazing and metabolism at the equator in the central Pacific: Implications for carbon and nitrogen fluxes. *Deep-Sea Research Part II*, 42(2–3), 735–756. [https://doi.org/10.1016/0967-0645\(95\)00036-P](https://doi.org/10.1016/0967-0645(95)00036-P)
- Davison, P. C., Checkley, D. M., Koslow, J. A., & Barlow, J. (2013). Carbon export mediated by mesopelagic fishes in the northeast Pacific Ocean. *Progress in Oceanography*, 116, 14–30. <https://doi.org/10.1016/j.pocean.2013.05.013>
- De Brabandere, L., Brion, N., Elskens, M., Baeyens, W., & Dehairs, F. (2007). Delta N-15 dynamics of ammonium and particulate nitrogen in a temperate eutrophic estuary. *Biogeochemistry*, 82(1), 1–14.
- Décima, M., Landry, M. R., Bradley, C. J., & Fogel, M. L. (2017). Alanine  $\delta^{15}\text{N}$  trophic fractionation in heterotrophic protists. *Limnology and Oceanography*, 62(5), 2308–2322. <https://doi.org/10.1002/lno.10567>
- Décima, M., Landry, M. R., & Rykaczewski, R. R. (2011). Broad-scale patterns in mesozooplankton biomass and grazing in the eastern equatorial Pacific. *Deep Sea Research, Part II*, 58(3-4), 387–399. <https://doi.org/10.1016/j.dsr2.2010.08.006>
- Décima, M., Landry, M. R., Stukel, M. R., Lopez-Lopez, L., & Krause, J. W. (2016). Mesozooplankton biomass and grazing in the Costa Rica Dome: Amplifying variability through the plankton food web. *Journal of Plankton Research*, 38(2), 317–330. <https://doi.org/10.1093/plankt/fbv091>
- Décima, M., Stukel, M. R., López-López, L., & Landry, M. R. (2019). The unique ecological role of pyrosomes in the Eastern Tropical Pacific. *Limnology and Oceanography*. <https://doi.org/10.1002/lno.11071>
- Del Giorgio, P. A., & Cole, J. J. (1998). Bacterial growth efficiency in natural aquatic systems. *Annual Review of Ecology and Systematics*, 29(1), 503–541. <https://doi.org/10.1146/annurev.ecolsys.29.1.503>
- Dilling, L., & Brzezinski, M. A. (2004). Quantifying marine snow as a food choice for zooplankton using stable silicon isotope tracers. *Journal of Plankton Research*, 26(9), 1105–1114. <https://doi.org/10.1093/plankt/fbh103>
- Dilling, L., Wilson, J., Steinberg, D., & Alldredge, A. (1998). Feeding by the euphausiid *Euphausia pacifica* and the copepod *Calanus pacificus* on marine snow. *Marine Ecology: Progress Series*, 170, 189–201. <https://doi.org/10.3354/meps170189>
- Dore, J. E., Brum, L. M. Jr., & Tupas, D. M. K. (2002). Seasonal and interannual variability in sources of nitrogen supporting export in the oligotrophic subtropical north Pacific Ocean. *Limnology and Oceanography*, 47(6), 1595–1607. <https://doi.org/10.4319/lo.2002.47.6.1595>
- Ducklow, H. W., Stukel, M. R., Eveleth, R., Jickells, T., Schofield, O., Doney, S., et al. (2018). Spring-summer net community production, new production, particle export and related water column biogeochemical processes in the marginal sea ice zone of the Western Antarctic peninsula 2012–2014. *Philosophical Transactions of the Royal Society of London A*, 376(2122). <https://doi.org/10.1098/rsta.2017.0177>
- Dunne, J. P., Murray, J. W., Rodier, M., & Hansell, D. A. (2000). Export flux in the western and central equatorial Pacific: Zonal and temporal variability. *Deep-Sea Research Part I*, 47(5), 901–936. [https://doi.org/10.1016/S0967-0637\(99\)00089-8](https://doi.org/10.1016/S0967-0637(99)00089-8)
- Eichinger, M., Poggiale, J. C., Van Wambeke, F., Lefevre, D., & Sempere, R. (2006). Modelling DOC assimilation and bacterial growth efficiency in biodegradation experiments: A case study in the Northeast Atlantic Ocean. *Aquatic Microbial Ecology*, 43(2), 139–151. <https://doi.org/10.3354/ame043139>
- Elliott, D. T., Harris, C. K., & Tang, K. W. (2010). Dead in the water: The fate of copepod carcasses in the York River estuary, Virginia. *Limnology and Oceanography*, 55(5), 1821–1834. <https://doi.org/10.4319/lo.2010.55.5.1821>
- Eppley, R. W., & Peterson, B. J. (1979). Particulate organic matter flux and planktonic new production in the deep ocean. *Nature*, 282(5740), 677–680. <https://doi.org/10.1038/282677a0>

- Estapa, M. L., Siegel, D. A., Buesseler, K. O., Stanley, R. H. R., Lomas, M. W., & Nelson, N. B. (2015). Decoupling of net community and export production on submesoscales. *Global Biogeochemical Cycles*, *29*, 1266–1282. <https://doi.org/10.1002/2014GB004913>
- Fiedler, P. C. (2002). The annual cycle and biological effects of the Costa Rica Dome. *Deep-Sea Research Part I*, *49*(2), 321–338. [https://doi.org/10.1016/S0967-0637\(01\)00057-7](https://doi.org/10.1016/S0967-0637(01)00057-7)
- Fleming, N. E. C., Harrod, C., Griffin, D. C., Newton, J., & Houghton, J. D. R. (2014). Scyphozoan jellyfish provide short-term reproductive habitat for hyperiid amphipods in a temperate near-shore environment. *Marine Ecology: Progress Series*, *510*, 229–240. <https://doi.org/10.3354/meps10896>
- Frangoulis, C., Skiris, N., Lepoint, G., Elkalay, K., Goffart, A., Pinnegar, J. K., & Hecq, J. H. (2011). Importance of copepod carcasses versus faecal pellets in the upper water column of an oligotrophic area. *Estuarine, Coastal and Shelf Science*, *92*(3), 456–463. <https://doi.org/10.1016/j.ecss.2011.02.005>
- Freibott, A., Taylor, A. G., Selph, K. E., Liu, H., Zhang, W., & Landry, M. R. (2016). Biomass and composition of protistan grazers and heterotrophic bacteria in the Costa Rica Dome during summer 2010. *Journal of Plankton Research*, *38*(2), 230–243. <https://doi.org/10.1093/plankt/fbv107>
- Gowing, M. M., & Wishner, K. F. (1986). Trophic relationships of deep-sea calanoid copepods from the benthic boundary layer of the Santa Catalina Basin, California. *Deep-Sea Research*, *33*(7), 939–961. [https://doi.org/10.1016/0198-0149\(86\)90008-7](https://doi.org/10.1016/0198-0149(86)90008-7)
- Gutierrez-Rodriguez, A., Decima, M., Popp, B. N., & Landry, M. R. (2014). Isotopic invisibility of protozoan trophic steps in marine food webs. *Limnology and Oceanography*, *59*(5), 1590–1598. <https://doi.org/10.4319/lo.2014.59.5.1590>
- Hannides, C. C. S., Landry, M. R., Benitez-Nelson, C. R., Styles, R. M., Montoya, J. P., & Karl, D. M. (2009). Export stoichiometry and migrant-mediated flux of phosphorus in the North Pacific subtropical gyre. *Deep-Sea Research Part I*, *56*(1), 73–88. <https://doi.org/10.1016/j.dsr.2008.08.003>
- Hansen, P. J., Bjornsen, P. K., & Hansen, B. W. (1997). Zooplankton grazing and growth: Scaling within the 2–2,000- $\mu$ m body size range. *Limnology and Oceanography*, *42*(4), 687–704. <https://doi.org/10.4319/lo.1997.42.4.0687>
- Hidaka, K., Kawaguchi, K., Murakami, M., & Takahashi, M. (2001). Downward transport of organic carbon by diel migratory micronekton in the western equatorial Pacific: Its quantitative and qualitative importance. *Deep-Sea Research Part I*, *48*(8), 1923–1939.
- Hobson, K. A., Fisk, A., Karnovsky, N., Holst, M., Gagnon, J. M., & Fortier, M. (2002). A stable isotope ( $\delta$ -C-13,  $\delta$ -N-15) model for the north water food web: Implications for evaluating trophodynamics and the flow of energy and contaminants. *Deep-Sea Research Part II*, *49*(22–23), 5131–5150. [https://doi.org/10.1016/S0967-0645\(02\)00182-0](https://doi.org/10.1016/S0967-0645(02)00182-0)
- Hoch, M. P., Snyder, R. A., Cifuentes, L. A., & Coffin, R. B. (1996). Stable isotope dynamics of nitrogen recycled during interactions among marine bacteria and protists. *Marine Ecology: Progress Series*, *132*(1–3), 229–239. <https://doi.org/10.3354/meps132229>
- Hofmann, E. E., Busalacchi, A. J., & Obrien, J. J. (1981). Wind generation of the Costa Rica Dome. *Science*, *214*(4520), 552–554. <https://doi.org/10.1126/science.214.4520.552>
- Horrigan, S., Montoya, J., Nevins, J., & McCarthy, J. (1990). Natural isotopic composition of dissolved inorganic nitrogen in the Chesapeake Bay. *Estuarine, Coastal and Shelf Science*, *30*(4), 393–410. [https://doi.org/10.1016/0272-7714\(90\)90005-C](https://doi.org/10.1016/0272-7714(90)90005-C)
- Houde, E. D., & Schekter, R. C. (1983). Oxygen uptake and comparative energetics among eggs and larvae of three subtropical marine fishes. *Marine Biology*, *72*(3), 283–293. <https://doi.org/10.1007/BF00396834>
- Ikeda, T. (1985). Metabolic rates of epipelagic marine zooplankton as a function of body mass and temperature. *Marine Biology*, *85*(1), 1–11. <https://doi.org/10.1007/BF00396409>
- Kones, J. K., Soetaert, K., van Oevelen, D., & Owino, J. O. (2009). Are network indices robust indicators of food web functioning? A Monte Carlo approach. *Ecological Modelling*, *220*(3), 370–382. <https://doi.org/10.1016/j.ecolmodel.2008.10.012>
- Kones, J. K., Soetaert, K., van Oevelen, D., Owino, J. O., & Mavuti, K. (2006). Gaining insight into food webs reconstructed by the inverse method. *Journal of Marine Systems*, *60*(1–2), 153–166. <https://doi.org/10.1016/j.jmarsys.2005.12.002>
- Krause, J. W., Stukel, M. R., Taylor, A. G., Taniguchi, D. A., De Verneil, A., & Landry, M. R. (2016). Net biogenic silica production and the contribution of diatoms to new production and organic matter export in the Costa Rica Dome ecosystem. *Journal of Plankton Research*, *38*(2), 216–229.
- Landry, M. R., Al-Mutairi, H., Selph, K. E., Christensen, S., & Nunnery, S. (2001). Seasonal patterns of mesozooplankton abundance and biomass at station ALOHA. *Deep-Sea Research Part II*, *48*(8–9), 2037–2061. [https://doi.org/10.1016/S0967-0645\(00\)00172-7](https://doi.org/10.1016/S0967-0645(00)00172-7)
- Landry, M. R., De Verneil, A., Goes, J. I., & Moffett, J. W. (2016). Plankton dynamics and biogeochemical fluxes in the Costa Rica Dome: Introduction to the CRD flux and zinc experiments. *Journal of Plankton Research*, *38*(2), 167–182. <https://doi.org/10.1093/plankt/fbv103>
- Landry, M. R., & Décima, M. R. (2017). Protistan microzooplankton and the trophic position of tuna: Quantifying the trophic link between micro- and mesozooplankton in marine foodwebs. *ICES Journal of Marine Science*, *74*(7), 1885–1892. <https://doi.org/10.1093/icesjms/fsx006>
- Landry, M. R., Ohman, M. D., Goericke, R., Stukel, M. R., & Tsyklevich, K. (2009). Lagrangian studies of phytoplankton growth and grazing relationships in a coastal upwelling ecosystem off Southern California. *Progress in Oceanography*, *83*(1–4), 208–216. <https://doi.org/10.1016/j.pocean.2009.07.026>
- Landry, M. R., Selph, K. E., Decima, M., Gutierrez-Rodriguez, A., Stukel, M. R., Taylor, A. G., & Pasulka, A. L. (2016). Phytoplankton production and grazing balances in the Costa Rica Dome. *Journal of Plankton Research*, *38*(2), 366–379. <https://doi.org/10.1093/plankt/fbv089>
- Le Borgne, R., & Rodier, M. (1997). Net zooplankton and the biological pump: A comparison between the oligotrophic and mesotrophic equatorial Pacific. *Deep-Sea Research Part II*, *44*(9–10), 2003–2023. [https://doi.org/10.1016/S0967-0645\(97\)00034-9](https://doi.org/10.1016/S0967-0645(97)00034-9)
- Levy, M., Bopp, L., Karleskind, P., Resplandy, L., Ethe, C., & Pinsard, F. (2013). Physical pathways for carbon transfers between the surface mixed layer and the ocean interior. *Global Biogeochemical Cycles*, *27*, 1001–1012. <https://doi.org/10.1002/gbc.20092>
- Li, W. K. W., Rao, D. V. S., Harrison, W. G., Smith, J. C., Cullen, J. J., Irwin, B., & Platt, T. (1983). Autotrophic picoplankton in the tropical ocean. *Science*, *219*(4582), 292–295. <https://doi.org/10.1126/science.219.4582.292>
- Lipschultz, F. (2001). A time-series assessment of the nitrogen cycle at BATS. *Deep-Sea Research Part II*, *48*(8–9), 1897–1924. [https://doi.org/10.1016/S0967-0645\(00\)00168-5](https://doi.org/10.1016/S0967-0645(00)00168-5)
- Lomas, M. W., Bates, N. R., Johnson, R. J., Knap, A. H., Steinberg, D. K., & Carlson, C. A. (2013). Two decades and counting: 24-years of sustained open ocean biogeochemical measurements in the Sargasso Sea. *Deep-Sea Research Part II*, *93*, 16–32. <https://doi.org/10.1016/j.dsr2.2013.01.008>
- Longhurst, A. R., Bedo, A. W., Harrison, W. G., Head, E. J. H., & Sameoto, D. D. (1990). Vertical flux of respiratory carbon by oceanic diel migrant biota. *Deep-Sea Research*, *37*(4), 685–694. [https://doi.org/10.1016/0198-0149\(90\)90098-G](https://doi.org/10.1016/0198-0149(90)90098-G)
- Mayor, D. J., Cook, K., Thornton, B., Walsham, P., Witte, U. F. M., Zuur, A. F., & Anderson, T. R. (2011). Absorption efficiencies and basal turnover of C, N and fatty acids in a marine Calanoid copepod. *Functional Ecology*, *25*(3), 509–518. <https://doi.org/10.1111/j.1365-2435.2010.01791.x>

- McCarthy, J. J., Garside, C., Nevins, J. L., & Barber, R. T. (1996). New production along 140°W in the equatorial Pacific during and following the 1992 El Niño event. *Deep-Sea Research Part II*, 43(4–6), 1065–1093. [https://doi.org/10.1016/0967-0645\(96\)00022-7](https://doi.org/10.1016/0967-0645(96)00022-7)
- Mino, Y., Sukigara, C., Honda, M. C., Kawakami, H., Matsumoto, K., Wakita, M., et al. (2016). Seasonal variations in the nitrogen isotopic composition of settling particles at station K2 in the western subarctic North Pacific. *Journal of Oceanography*, 72(6), 819–836. <https://doi.org/10.1007/s10872-016-0381-1>
- Möbius, J. (2013). Isotope fractionation during nitrogen remineralization (ammonification): Implications for nitrogen isotope biogeochemistry. *Geochimica et Cosmochimica Acta*, 105(Supplement C), 422–432. <https://doi.org/10.1016/j.gca.2012.11.048>
- Montoya, J. P. (2008). Chapter 29—Nitrogen stable isotopes in marine environments. In D. G. Capone, D. A. Bronk, M. R. Mulholland, & E. J. Carpenter (Eds.), *Nitrogen in the Marine Environment* (2nd ed., pp. 1277–1302). San Diego, CA: Academic Press. <https://doi.org/10.1016/B978-0-12-372522-6.00029-3>
- Montoya, J. P., Carpenter, E. J., & Capone, D. G. (2002). Nitrogen fixation and nitrogen isotope abundances in zooplankton of the oligotrophic North Atlantic. *Limnology and Oceanography*, 47(6), 1617–1628. <https://doi.org/10.4319/lo.2002.47.6.1617>
- Montoya, J. P., Horrigan, S. G., & McCarthy, J. J. (1991). Rapid, storm-induced changes in the natural abundance of N-15 in a planktonic ecosystem, Chesapeake Bay, USA. *Geochimica et Cosmochimica Acta*, 55(12), 3627–3638. [https://doi.org/10.1016/0016-7037\(91\)90060-1](https://doi.org/10.1016/0016-7037(91)90060-1)
- Montoya, J. P., & McCarthy, J. J. (1995). Isotopic fractionation during nitrate uptake by phytoplankton grown in continuous culture. *Journal of Plankton Research*, 17(3), 439–464. <https://doi.org/10.1093/plankt/17.3.439>
- Needoba, J. A., Waser, N., Harrison, P., & Calvert, S. (2003). Nitrogen isotope fractionation in 12 species of marine phytoplankton during growth on nitrate. *Marine Ecology: Progress Series*, 255, 81–91. <https://doi.org/10.3354/meps255081>
- Omand, M. M., A. E., D'Asaro, C. M., Lee, M. J., Perry, N., Briggs, I. C., & Mahadevan, A. (2015). Eddy-driven subduction exports particulate organic carbon from the spring bloom. *Science*, 348(6231), 222–225. <https://doi.org/10.1126/science.1260062>
- Paffenhöfer, G. A., & Strickland, J. D. (1970). A note on feeding of *Calanus helgolandicus* on detritus. *Marine Biology*, 5(2), 97–99. <https://doi.org/10.1007/BF00352591>
- Park, J.-I., Kang, C.-K., & Suh, H.-L. (2011). Ontogenetic diet shift in the euphausiid *Euphausia pacifica* quantified using stable isotope analysis. *Marine Ecology: Progress Series*, 429, 103–109. <https://doi.org/10.3354/meps09091>
- Parker, A. E., Wilkerson, F. P., Dugdale, R. C., Marchi, A., & Hogue, V. (2011). Patterns of nitrogen concentration and uptake by two phytoplankton size-classes in the equatorial Pacific Ocean (110°W–140°W) during 2004 and 2005. *Deep-Sea Research Part II*, 58(3–4), 417–433. <https://doi.org/10.1016/j.dsr2.2010.08.013>
- Pennock, J. R., Velinsky, D. J., Ludlam, J. M., Sharp, J. H., & Fogel, M. L. (1996). Isotopic fractionation of ammonium and nitrate during uptake by *Skeletonema costatum*: Implications for delta N-15 dynamics under bloom conditions. *Limnology and Oceanography*, 41(3), 451–459. <https://doi.org/10.4319/lo.1996.41.3.0451>
- Post, D. M. (2002). Using stable isotopes to estimate trophic position: Models, methods, and assumptions. *Ecology*, 83(3), 703–718. [https://doi.org/10.1890/0012-9658\(2002\)083\[0703:USITET\]2.0.CO;2](https://doi.org/10.1890/0012-9658(2002)083[0703:USITET]2.0.CO;2)
- Rau, G. H., Ohman, M. D., & Pierrot-Bults, A. (2003). Linking nitrogen dynamics to climate variability off central California: A 51 year record based on N-15/N-14 in CalCOFI zooplankton. *Deep-Sea Research Part II*, 50(14–16), 2431–2447. [https://doi.org/10.1016/S0967-0645\(03\)00128-0](https://doi.org/10.1016/S0967-0645(03)00128-0)
- Reilly, S. B., & Thayer, V. G. (1990). Blue whale (*Balaenoptera musculus*) distribution in the eastern tropical Pacific. *Marine Mammal Science*, 6(4), 265–277. <https://doi.org/10.1111/j.1748-7692.1990.tb00357.x>
- Richardson, T. L., Jackson, G. A., Ducklow, H. W., & Roman, M. R. (2004). Carbon fluxes through food webs of the eastern equatorial Pacific: An inverse approach. *Deep-Sea Research Part I*, 51(9), 1245–1274. <https://doi.org/10.1016/j.dsr.2004.05.005>
- Robinson, D. (2001). Delta N-15 as an integrator of the nitrogen cycle. *Trends in Ecology & Evolution*, 16(3), 153–162. [https://doi.org/10.1016/S0169-5347\(00\)02098-X](https://doi.org/10.1016/S0169-5347(00)02098-X)
- Roman, M. R. (1984a). Ingestion of detritus and microheterotrophs by pelagic marine zooplankton. *Bulletin of Marine Science*, 35(3), 477–494.
- Roman, M. R. (1984b). Utilization of detritus by the copepod *Acartia tonsa*. *Limnology and Oceanography*, 29(5), 949–959. <https://doi.org/10.4319/lo.1984.29.5.0949>
- Roman, M. R., Dam, H. G., Le Borgne, R., & Zhang, X. (2002). Latitudinal comparisons of equatorial Pacific zooplankton. *Deep-Sea Research Part II*, 49(13–14), 2695–2711. [https://doi.org/10.1016/S0967-0645\(02\)00054-1](https://doi.org/10.1016/S0967-0645(02)00054-1)
- Roman, M. R., & Gauzens, A. L. (1997). Copepod grazing in the equatorial Pacific. *Limnology and Oceanography*, 42(4), 623–634. <https://doi.org/10.4319/lo.1997.42.4.0623>
- Roman, M. R., & Tenore, K. R. (1984). Detritus dynamics in aquatic ecosystems: An overview. *Bulletin of Marine Science*, 35(3), 257–260.
- Saint-Béat, B., Vézina, A. F., Asmus, R., Asmus, H., & Niquil, N. (2013). The mean function provides robustness to linear inverse modelling flow estimation in food webs: A comparison of functions derived from statistics and ecological theories. *Ecological Modelling*, 258, 53–64. <https://doi.org/10.1016/j.ecolmodel.2013.01.023>
- Saito, M. A., Rocab, G., & Moffett, J. W. (2005). Production of cobalt binding ligands in a *Synechococcus* feature at the Costa Rica upwelling dome. *Limnology and Oceanography*, 50(1), 279–290. <https://doi.org/10.4319/lo.2005.50.1.0279>
- Sambrotto, R. N. (2001). Nitrogen production in the northern Arabian Sea during the spring intermonsoon and southwest monsoon seasons. *Deep-Sea Research Part II*, 48(6–7), 1173–1198. [https://doi.org/10.1016/S0967-0645\(00\)00135-1](https://doi.org/10.1016/S0967-0645(00)00135-1)
- Selph, K. E., Landry, M. R., Taylor, A. G., Gutierrez-Rodriguez, A., Stukel, M. R., Wokuluk, J., & Pasulka, A. (2016). Phytoplankton production and taxon-specific growth rates in the Costa Rica Dome. *Journal of Plankton Research*, 38(2), 199–215. <https://doi.org/10.1093/plankt/fbv063>
- Selph, K. E., Landry, M. R., Taylor, A. G., Yang, E. J., Measures, C. I., Yang, J. J., et al. (2011). Spatially-resolved taxon-specific phytoplankton production and grazing dynamics in relation to iron distributions in the equatorial Pacific between 110 and 140°W. *Deep-Sea Research Part II*, 58(3–4), 358–377. <https://doi.org/10.1016/j.dsr2.2010.08.014>
- Sigman, D. M., Altabet, M. A., McCorkle, D. C., Francois, R., & Fischer, G. (1999). The delta N-15 of nitrate in the Southern Ocean: Consumption of nitrate in surface waters. *Global Biogeochemical Cycles*, 13(4), 1149–1166. <https://doi.org/10.1029/1999GB000038>
- Smith, K. L. Jr., Sherman, A. D., Huffard, C. L., McGill, P. R., Henthorn, R., Von Thun, S., et al. (2014). Large salp bloom export from the upper ocean and benthic community response in the abyssal northeast Pacific: Day to week resolution. *Limnology and Oceanography*, 59(3), 745–757. <https://doi.org/10.4319/lo.2014.59.3.0745>
- Soetaert, K., Van den Meersche, K., & van Oevelen, D. (2009). limSolve: Solving linear inverse models, in *R package version*, edited.
- Steffan, S. A., Chikaraishi, Y., Currie, C. R., Horn, H., Gaines-Day, H. R., Pauli, J. N., et al. (2015). Microbes are trophic analogs of animals. *Proceedings of the National Academy of Sciences*, 112(49), 15,119–15,124. <https://doi.org/10.1073/pnas.1508782112>
- Steinberg, D. K., Van Mooy, B. A. S., Buesseler, K. O., Boyd, P. W., Kobari, T., & Karl, D. M. (2008). Bacterial vs. zooplankton control of sinking particle flux in the ocean's twilight zone. *Limnology and Oceanography*, 53(4), 1327–1338. <https://doi.org/10.4319/lo.2008.53.4.1327>

- Straille, D. (1997). Gross growth efficiencies of protozoan and metazoan zooplankton and their dependence on food concentration, predator-prey weight ratio, and taxonomic group. *Limnology and Oceanography*, *42*(6), 1375–1385. <https://doi.org/10.4319/lo.1997.42.6.1375>
- Stukel, M. R., Aluwihare, L. I., Barbeau, K. A., Chekalyuk, A. M., Goericke, R., Miller, A. J., et al. (2017). Mesoscale ocean fronts enhance carbon export due to gravitational sinking and subduction. *Proceedings of the National Academy of Sciences*, *114*(6), 1252–1257. <https://doi.org/10.1073/pnas.1609435114>
- Stukel, M. R., Asher, E., Coutos, N., Schofield, O., Strebel, S., Tortell, P. D., & Ducklow, H. W. (2015). The imbalance of new and export production in the western Antarctic peninsula, a potentially "leaky" ecosystem. *Global Biogeochemical Cycles*, *29*, 1400–1420. <https://doi.org/10.1002/2015GB005211>
- Stukel, M. R., Benitez-Nelson, C., Décima, M., Taylor, A. G., Buchwald, C., & Landry, M. R. (2016). The biological pump in the Costa Rica Dome: An open ocean upwelling system with high new production and low export. *Journal of Plankton Research*, *38*(2), 348–365. <https://doi.org/10.1093/plankt/fbv097>
- Stukel, M. R., Décima, M., Selph, K. E., Taniguchi, D. A. A., & Landry, M. R. (2013). The role of *Synechococcus* in vertical flux in the Costa Rica upwelling dome. *Progress in Oceanography*, *112–113*, 49–59. <https://doi.org/10.1016/j.pocean.2013.04.003>
- Stukel, M. R., & Ducklow, H. W. (2017). Stirring up the biological pump: Vertical mixing and carbon export in the Southern Ocean. *Global Biogeochemical Cycles*, *31*, 1420–1434. <https://doi.org/10.1002/2017GB005652>
- Stukel, M. R., Kelly, T. B., & Decima, M. R. (2018). A new approach for incorporating nitrogen isotope measurements into linear inverse ecosystem models with Markov Chain Monte Carlo sampling. *PLoS One*, *13*(6), e0199123. <https://doi.org/10.1371/journal.pone.0199123>
- Stukel, M. R., & Landry, M. R. (2010). Contribution of picophytoplankton to carbon export in the equatorial Pacific: A re-assessment of food-web flux inferences from inverse models. *Limnology and Oceanography*, *55*(6), 2669–2685. <https://doi.org/10.4319/lo.2010.55.6.2669>
- Stukel, M. R., Landry, M. R., Ohman, M. D., Goericke, R., Samo, T., & Benitez-Nelson, C. R. (2012). Do inverse ecosystem models accurately reconstruct plankton trophic flows? Comparing two solution methods using field data from the California Current. *Journal of Marine Systems*, *91*(1), 20–33. <https://doi.org/10.1016/j.jmarsys.2011.09.004>
- Stukel, M. R., Landry, M. R., & Selph, K. E. (2011). Nanoplankton mixotrophy in the eastern equatorial Pacific. *Deep-Sea Research Part II*, *58*(3–4), 378–386. <https://doi.org/10.1016/j.dsr2.2010.08.016>
- Stukel, M. R., Ohman, M. D., Benitez-Nelson, C. R., & Landry, M. R. (2013). Contributions of mesozooplankton to vertical carbon export in a coastal upwelling system. *Marine Ecology: Progress Series*, *491*, 47–65. <https://doi.org/10.3354/meps10453>
- Tameler, T., Søreide, J. E., Hop, H., & Carroll, M. L. (2006). Fractionation of stable isotopes in the Arctic marine copepod *Calanus glacialis*: Effects on the isotopic composition of marine particulate organic matter. *Journal of Experimental Marine Biology and Ecology*, *333*(2), 231–240. <https://doi.org/10.1016/j.jembe.2006.01.001>
- Taylor, A. G., Landry, M. R., Freibott, A., Selph, K. E., & Gutierrez-Rodriguez, A. (2016). Patterns of microbial community biomass, composition and HPLC diagnostic pigments in the Costa Rica upwelling dome. *Journal of Plankton Research*, *38*(2), 183–198. <https://doi.org/10.1093/plankt/fbv086>
- Taylor, A. G., Landry, M. R., Selph, K. E., & Yang, E. J. (2011). Microplankton community structure in the eastern equatorial Pacific. *Deep-Sea Research Part II*, *58*(3–4), 342–357. <https://doi.org/10.1016/j.dsr2.2010.08.017>
- Van den Meersche, K., Soetaert, K., & Van Oevelen, D. (2009). xSample(): An R function for sampling linear inverse problems. *Journal of Statistical Software, Code Snippets*, *30*(1), 1–15.
- van Oevelen, D., Van den Meersche, K., Meysman, F. J. R., Soetaert, K., Middelburg, J. J., & Vezina, A. F. (2010). Quantifying food web flows using linear inverse models. *Ecosystems*, *13*(1), 32–45. <https://doi.org/10.1007/s10021-009-9297-6>
- Vézina, A. F., & Pahlow, M. (2003). Reconstruction of ecosystem flows using inverse methods: How well do they work? *Journal of Marine Systems*, *40*, 55–77.
- Vézina, A. F., & Platt, T. (1988). Food web dynamics in the ocean .1. Best estimates of flow networks using inverse methods. *Marine Ecology: Progress Series*, *42*(3), 269–287. <https://doi.org/10.3354/meps042269>
- Vilchis, L. I., Ballance, L. T., & Fiedler, P. C. (2006). Pelagic habitat of seabirds in the eastern tropical Pacific: Effects of foraging ecology on habitat selection. *Marine Ecology: Progress Series*, *315*, 279–292. <https://doi.org/10.3354/meps315279>
- Voss, M., Nausch, G., & Montoya, J. P. (1997). Nitrogen stable isotope dynamics in the central Baltic Sea: Influence of deep-water renewal on the N-cycle changes. *Marine Ecology: Progress Series*, *158*, 11–21. <https://doi.org/10.3354/meps158011>
- Waser, N. A., Yin, K. D., Yu, Z. M., Tada, K., Harrison, P. J., Turpin, D. H., & Calvert, S. E. (1998). Nitrogen isotope fractionation during nitrate, ammonium and urea uptake by marine diatoms and coccolithophores under various conditions of N availability. *Marine Ecology: Progress Series*, *169*, 29–41. <https://doi.org/10.3354/meps169029>
- Wilson, S. E., & Steinberg, D. K. (2010). Autotrophic picoplankton in mesozooplankton guts: Evidence of aggregate feeding in the mesopelagic zone and export of small phytoplankton. *Marine Ecology: Progress Series*, *412*, 11–27. <https://doi.org/10.3354/meps08648>
- Wilson, S. E., Steinberg, D. K., Chu, F. L. E., & Bishop, J. K. B. (2010). Feeding ecology of mesopelagic zooplankton of the subtropical and subarctic north Pacific Ocean determined with fatty acid biomarkers. *Deep-Sea Research Part I*, *57*(10), 1278–1294. <https://doi.org/10.1016/j.dsr.2010.07.005>
- Wu, J. P., Calvert, S. E., & Wong, C. S. (1997). Nitrogen isotope variations in the subarctic northeast Pacific: Relationships to nitrate utilization and trophic structure. *Deep-Sea Research Part I*, *44*(2), 287–314. [https://doi.org/10.1016/S0967-0637\(96\)00099-4](https://doi.org/10.1016/S0967-0637(96)00099-4)
- Zhang, X. S., & Dam, H. G. (1997). Downward export of carbon by diel migrant mesozooplankton in the central equatorial Pacific. *Deep-Sea Research Part II*, *44*(9–10), 2191–2202. [https://doi.org/10.1016/S0967-0645\(97\)00060-X](https://doi.org/10.1016/S0967-0645(97)00060-X)